Estimating the Interest Rate Trend in a Shadow Rate Term Structure Model

Yang Han* Jun Ma†

March 22, 2023

Abstract

We propose a shadow rate no-arbitrage dynamic term structure model with drifting trends to estimate the long run trend of real interest rate using data from the U.S., the U.K., and Germany from January 1972 to April/March 2022. The interest rate trends of all three countries have declined since the 1990s, and there is strong co-movement among them. We document evidence that our model can provide better yield forecasts than existing models. The term premium estimates of our model are stationary and are positively correlated with inflation uncertainty measures, corroborating the findings of Wright (2011).

JEL Classification: E43; E44; E47

Keywords: interest rate trend; no-arbitrage dynamic term structural model; zero lower bound; term premium

*School of Banking and Finance, University of International Business and Economics, No.10 Huixin East Street, Beijing 100029, China. E-mail: hanyang@uibe.edu.cn

†Department of Economics, Northeastern University, 360 Huntington Avenue, Boston, MA 02115. E-mail: ju.ma@northeastern.edu

1 Introduction

A consensus has emerged that there has been a declining trend in the interest rate since the early 1990s in the U.S. as well as several major industrialized economies (Laubach and Williams (2003), Summers (2016), Hamilton et al. (2016), Holston et al. (2017), etc.) While the advanced economies had operated under the regime of extremely low interest rates for over a decade in the wake of the 2008-2009 financial crisis, which appeared to be reinforced only by the COVID pandemic, the most recent episode of skyrocketing inflation and the resulting aggressive monetary policy tightening undoubtedly raises the question of whether this low interest rate regime will persist. Accurately tracking the long-run trend of the real interest rate is instrumental for both monetary policy conduct and asset management, and thus of great interest to both academics and industry practitioners.

We propose a novel shadow rate dynamic term structure model (SDTSM) with drifting trends to better estimate the long-run trend of the real interest rate and improve yield curve forecasts. Our model explicitly accounts for both the lower bound constraint of the short-term nominal interest rate in the spirit of Wu and Xia (2016) and the low-frequency movement of the interest rate by following Bauer and Rudebusch (2020). Under the conventional notion that all permanent shocks to real interest rates are derived from real shocks, our trend estimate of the real interest rate can also be taken as a trend estimate of the natural rate of real interest, which is key to assessing the monetary policy stance (Barsky et al. (2014)).

A growing body of literature has documented this declining interest rate trend and has attempted to shed light on its underlying driving forces. For example, Laubach and Williams (2016) and Laubach and Williams (2003) apply a multivariate unobserved components model consisting of several macroeconomic variables and provide a popular trend estimate of the natural rate in the United States. They find that the U.S. natural rate has trended sharply

downward since the Great Recession, to a near-zero level. Their methodology directly connects a slower trend of output growth to the declining natural rate trend, and thus, is unambiguous about its source. In a related study, Holston et al. (2017) employs a similar approach and presents evidence that the United States, Canada, the Euro Area, and the United Kingdom all witnessed large declines in their natural rate trends, together with large declines in output growth trends during the same time period. In another notable example, Del Negro et al. (2017) estimates the interest rate trend in a multivariate unobserved components model comprising short- and long-term bond yields and discover a similarly declining interest rate trend in the United States, but their study highlights the important role of the convenience yield of treasury bonds as the driving force.

Estimating and tracking the long-run trend of interest rates in environments with extremely low short-term nominal interest rates near their effective lower bounds pose serious challenges. In models such as that of Laubach and Williams (2003), the small size of trend variations in output growth has already plagued the estimation with the "pile-up" issue (Stock (1994)), leading to a two-step approach. The near-zero short-term nominal interest rate since the Great Recession further exacerbates this identification issue, particularly in models that rely primarily on the short end of the yield curve (Lubik and Matthes (2015)). Therefore, it is not surprising that long-term interest rates are increasingly brought in to help forecast interest rate trends (e.g., see Del Negro et al. (2017)and Johannsen and Mertens (2021)). However, the well-documented failure of the expectation hypothesis suggests that a model that can coherently and flexibly deal with term premiums is crucial to correctly extract interest rate trends from long-term yields.

To directly address this issue, this study provides an alternative estimate of interest rate trends by exploring a broad set of yield data in the Treasury bond market and carefully handling the zero lower bound (ZLB). To this end, we develop a no-arbitrage dynamic term structure model (DTSM) that features a shifting endpoint in the spirit of Kozicki and Tins-

ley (2001) by following Bauer and Rudebusch (2020) and explicitly accounts for the ZLB by employing the shadow rate approach akin to Wu and Xia (2016, 2020) and Krippner (2015). The proposed approach has several advantages. First, as demonstrated in Wu and Zhang (2019), the shadow rate summarizes the overall financial market condition including both short-term and long-term lendings, the role of the latter being particularly important during the ZLB period. By adopting a common approach of defining the interest rate trend as the long-run forecast, namely the Beveridge-Nelson trend, of the shadow rate, our model works as a device to effectively transform the long-run forecast of macroeconomic equilibrium information embodied in the entire yield curve into a single series. The resulting more variable shadow rate lends itself to improved identification of its trend. Second, our approach harnesses the entire yield curve and exploits no-arbitrage restrictions to efficiently extract information. This sets us apart from Del Negro et al. (2017) and Johannsen and Mertens (2021), who select a few yields and do not impose no-arbitrage restrictions[1]. Notably, Christensen and Rudebusch (2019) directly extract a long-run forecast of the real interest rate from a no-arbitrage dynamic term structure model using Treasury Inflation Protected Security (TIPS) market data. However, TIPS yields are known to contain variable liquidity premiums, and despite their careful modeling of this component, they necessarily introduce additional sources of model misspecifications.

Third, in contrast to models that rely primarily on macroeconomic variables, we provide rich information in the Treasury bond market to identify the slow-moving interest rate trend in order to improve estimation efficiency. Estimates from models using primarily macroeconomic variables are often criticized because they are subject to data revisions and thus unreliable for policy guidance in real time (see Orphanides (2001) and Orphanides and van

[1]Many studies, with the exception of Johannsen and Mertens (2021), choose to drop the short-term interest rate by treating them as missing variables and switching to long-term interest rates during the ZLB period. Nevertheless, this practice is not innocuous given the important role of the time-varying term premium.

Norden (2002)). On the other hand, financial market data reflect more directly and timely market participants' views of the economy and are forward looking. Finally, our approach avoids restricting the interest rate trend movement to any specific macroeconomic variables or structural model, and thus remains agnostic about the underlying driving forces. Although the literature has proposed several potential driving forces of the declining interest rate trend, including slower productivity growth (Laubach and Williams (2003)), secular stagnation (Summers (2016)), changing demographics (Carvalho et al. (2016) and Favero et al. (2016)), and convenience yield (Del Negro et al. (2017)), there is no consensus on the role of each factor (Hamilton et al. (2016) and Lunsford and West (2019)). Instead, our approach exploits information in the liquid Treasury bond market and utilizes no-arbitrage restrictions on bond price movements across maturities to efficiently estimate interest rate trends.

Our model is built upon a strand of literature that develops a no-arbitrage dynamic term structure model of interest rates. Specifically, our model extends the model proposed by Bauer and Rudebusch (2020) (BR hereafter), which introduces an unspanned stochastic trend of the short-term interest rate into the Gaussian DTSM, as in Duffee (2011) and Joslin et al. (2011). Most DTSMs assume a stationary physical process for the yield curve and thus often underestimate interest rate trend variations (Kim and Orphanides (2012) and Bauer et al. (2014)). By introducing a shifting endpoint into the DTSM in the spirit of Kozicki and Tinsley (2001), the BR model is a convenient device to robustly track the drifting interest rate trend. We introduce the shadow rate of Black (1995) into the BR model and derive an analytical form of the term structure of interest rates by exploiting the Gaussian feature of the BR model and following a strategy similar to those of Wu and Xia (2016) and Krippner (2015). To the best of our knowledge, our study is the first to explicitly account for issues pertaining to the ZLB when estimating interest rate trends in a DTSM.

The analytical solution greatly facilitates the model estimation. Following Wu and Xia

(2016), we apply the extended Kalman filter and estimate our DTSM model using treasury bond forward rates at maturities ranging from 3 months to 10 years in the sample spanning from January 1972 to April/March 2022 for the United States, the United Kingdom, and Germany. Following Bauer and Rudebusch (2020), we employ a Bayesian estimation procedure that strategically combines Gibbs sampling and Metropolis-Hasting algorithms to simulate the posterior distributions of model parameters and state variables.

Our main findings can be summarized as follows: (1) The long-run trends of real interest rates have been declining in all three countries since as early as the 1990s, and have all turned negative in recent years. Furthermore, there is strong co-movement among the three interest rate trends, corroborating the findings of Diebold et al. (2008) and Holston et al. (2017). (2) The out-of-sample forecast exercises indicate that our model can significantly improve the yield curve forecast based on the existing term structure models. (3) The estimated duration of the ZLB at each time point corresponds well with relevant macroeconomic events and monetary policy announcements. (4) The term premium estimates vary substantially over time, but remain quite stationary, similar to Kim and Orphanides (2012) and Bauer and Rudebusch (2020), and are significantly and positively correlated with inflation uncertainty measures, lending support to the findings of Wright (2011).

The remainder of this paper is organized as follows. Section 2 describes the proposed method. Section 3 presents the data and Section 4 describes the estimation methodology. Section 5 discusses empirical results. Finally, Section 6 concludes the paper.

2 Model Specification

2.1 A Shadow Rate DTSM with Unspanned Drifting Trends

Following the DTSM literature, we assume yields are driven by a small number of latent factors in X_t that follows a parsimonious time series dynamics. To deal with the high persistence in yields across all maturities due to drifting trends in interest rates (see Kim and Orphanides (2012)), we follow Bauer and Rudebusch (2020) to introduce two stochastic trends: real interest rate trend, r_t^*, and inflation trend, π_t^*, and employ the following Stock-Watson type of common-trend representation for X_t:

$$X_t = \bar{X} + \Gamma' \tau_t + \tilde{X}_t \tag{1}$$

$$\tilde{X}_t = \Phi \tilde{X}_{t-1} + \tilde{u}_t \tag{2}$$

$$\tau_t = \begin{pmatrix} r_t^* \\ \pi_t^* \end{pmatrix} = \begin{pmatrix} 1 & 0 \\ 0 & 1 \end{pmatrix} \begin{pmatrix} r_{t-1}^* \\ \pi_{t-1}^* \end{pmatrix} + \begin{pmatrix} \eta_{rt} \\ \eta_{\pi t} \end{pmatrix} \tag{3}$$

where all eigenvalues of Φ are within the unit circle. To the extend that the shocks $\tilde{u}_t, \eta_{rt}, \eta_{\pi t}$ are assumed to be $i.i.d.$ and mutually orthogonal, this is a somewhat restricted model in the sense of Morley et al. (2003). r_t^* and π_t^* are the Beveridge-Nelson trends of their corresponding variables: $r_t^* = \lim_{j\to\infty} E_t\left(r_{t+j}\right)$ and $\pi_t^* = \lim_{j\to\infty} E_t\left(\pi_{t+j}\right)$, where r_t is real interest rate, and π_t inflation rate. We discuss how to pin down π_t^* using inflation data in the next subsection. We use yields to identify nominal interest rate trend which can be used together with the long-run Fisher equation to back out real interest rate trend.

To proceed, we first specify the short-run nominal interest rate that is not subject to the ZLB, or the shadow rate s_t, to be an affine function of the latent factors:

$$s_t = \delta_0 + \delta_1' X_t \tag{4}$$

The large-scale monetary policy easing by major central banks around the world in

the wake of the 2008-2009 great financial crisis (GFC) have pushed short-term nominal interest rates in major advanced economies to levels around zero since then for more than a decade until very recently when the central banks started to lift rates to combat rising inflation. The fact that investors always have the option of holding cash earning zero interest places an effective lower bound, or the ZLB, on the interest rate level central banks can set[2]. Introducing this shadow rate s_t that is not bounded from below allows us to preserve technical tractability of the DTSM to a large extent. Following the approach in Black (1995), the actual short-term nominal rate (i_t) can be viewed as a sum of the shadow rate and the value of an option of holding cash:

$$i_t = s_t + max(-s_t, \underline{i}) \tag{5}$$

where $\underline{i}$ is the effective lower bound, and is 0 in most cases.

As in Johannsen and Mertens (2021), we define nominal interest rate trend, which is given by $r_t^* + \pi_t^*$ according to the long-run Fisher equation, as the long-run forecast of the shadow rate:

$$r_t^* + \pi_t^* = \lim_{j \to \infty} E_t s_{t+j} \tag{6}$$

Note this, together with equations (1) and (4), immediately implies the parameter restrictions pertaining to the trend identification: $\delta_0 + \delta_1' \bar{X} = 0$ and $\delta_1' \Gamma' [r_t^*, \pi_t^*]' = 1$.

As discussed in Wu and Xia (2016) the short-term nominal interest rate being stuck at the ZLB effectively shifts the information contained in the yield curve from the short end to the long end. The shadow rate can conveniently subsumes the information contained in the entire yield curve and better reflects both monetary policies and economic condition as

[2]Although ECB was able to lower its policy rate below zero, the amount of convenience premium investors are willing to pay still places an effective lower bound on its interest rate

perceived by market participants.

Following the DTSM literature, we include three factors in X_t that are assumed to be spanned by the yield curve. Evidence from Cieslak and Povala (2015),Coroneo et al. (2016), and Bauer and Rudebusch (2020) suggests that real interest trend and inflation trend may not be spanned by the yield curve. Therefore, these two factors are specified as unspanned (hidden) factors, akin to the approach in Bauer and Rudebusch (2020). Spanned factors directly drive the yield curve, whereas hidden factors do not contemporaneously determine yields. Instead, they enter the term structure model by interacting with the spanned factors in the physical process. Unlike the model in Joslin et al. (2014), where the unspanned factors are directly observable macroeconomic variables, all factors, including hidden factors, in our model are latent factors, similar to the model of Duffee (2011).

Rewritting the common-trend representation in equation (1) yields the following VAR(1) process for the latent factors under the physical (P) measure[3]:

$$\begin{pmatrix} X_t \\ r_t^* \\ \pi_t^* \end{pmatrix} = \begin{pmatrix} (I_3 - \Phi)\bar{X} \\ 0 \\ 0 \end{pmatrix} + \begin{pmatrix} \Phi & (I_3 - \Phi)\gamma & (I_3 - \Phi)\gamma \\ 0_{1\times 3} & 1 & 0 \\ 0_{1\times 3} & 0 & 1 \end{pmatrix} \begin{pmatrix} X_{t-1} \\ r_{t-1}^* \\ \pi_{t-1}^* \end{pmatrix} + \begin{pmatrix} u_t \\ \eta_{rt} \\ \eta_{\pi t} \end{pmatrix} \tag{7}$$

where $\tilde{u}_t = u_t - \gamma(\eta_{rt} + \eta_{\pi t})$. Note although the transitory shock $\tilde{u}_t$ is assumed to be orthogonal to the two trend shocks, the above structure implies that, in equation (7), the shock to the spanned factors X_t is correlated with the shocks to the hidden factors: $\text{cov}(u_t, \eta_{it}) = \gamma\sigma_{\eta i}^2$, and finally, $u_t \overset{iid}{\sim} N(0, \Sigma\Sigma')$.

Let $\tilde{Z}_t$ denote a vector containing all five latent factors, including spanned and hidden factors, with an arbitrary rotation. In a Gaussian DTSM, such as in Joslin et al. (2011),yields (Y_t) are affine in factors: $Y_t = a + \tilde{b} \cdot \tilde{Z}_t$, where the $n \times 1$ vector a and the $n \times 5$ matrix $\tilde{b}$ are

[3]We estimate a slightly restricted version of the model by assuming homogenous impacts of the two trends on interest rates: $\Gamma' = [\gamma, \gamma]$.

functions of the underlying model parameters under no-arbitrage restrictions, and n denotes the number of yields. Hidden factors exist if $\tilde{b}$ has a reduced rank. As noted by Duffee (2011), because all factors are latent, hidden factors can only be anchored by adopting a certain rotation. Specifically, the latent factors may be rotated using a full-rank matrix D such that $Y_t = a + b \cdot \bar{Z}_t$, where $b = \tilde{b} * D$ and $\bar{Z}_t = D^{-1} * \tilde{Z}_t = (X_t', r_t^*, \pi_t^*)'$, and the last two columns of b are all zeros because the last two factors in $\bar{Z}_t$ are hidden factors. We employ the same rotation as in Duffee (2011), and hence:

$$s_t = \delta_0 + (\delta_1', 0, 0)\ (X_t', r_t^*, \pi_t^*)' \tag{8}$$

where this equation is simply repeating equation (4) but to highlight the unspanned nature of the two trends: the hidden factors r_t^* and π_t^* do not further influence the shadow rate s_t conditioning on X_t. Consequently, as long as r_t^* and π_t^* are restricted to have zero impact on X_t, in the equivalent risk-neutral (Q) process under the no-arbitrage restriction, these two hidden factors are unspanned in the sense that their loadings on yields are exactly zero. As a result, the required Q-process for the latent factors is

$$\begin{pmatrix} X_t \\ r_t^* \\ \pi_t^* \end{pmatrix} = \begin{pmatrix} \mu^Q \\ \circ \\ \circ \end{pmatrix} + \begin{pmatrix} \Phi^Q & 0_{3\times1} & 0_{3\times1} \\ \circ & \circ & \circ \\ \circ & \circ & \circ \end{pmatrix} \begin{pmatrix} X_{t-1} \\ r_{t-1}^* \\ \pi_{t-1}^* \end{pmatrix} + \begin{pmatrix} u_t^Q \\ \circ \\ \circ \end{pmatrix} \tag{9}$$

The parameters at $\circ$ positions for the hidden factors are unidentified and thus, are excluded from the parameterization. The hidden factors result from the so-called "knife-edge" restriction, in which their impacts on the expected future values of X_t exactly offset their impacts on the risk price.

The above model implies a risk price (λ_t) that is affine in the latent factors:

$$\begin{aligned}\Sigma\lambda_t &= \lambda_0 + \lambda_1 \cdot (X_t', r_t^*, \pi_t^*)' \\ \lambda_0 &= (I_3 - \Phi)\bar{X} - \mu^Q \\ \lambda_1 &= \big(\Phi,\ (I_3 - \Phi)\gamma,\ (I_3 - \Phi)\gamma\big) - (\Phi^Q,\ 0_{3\times1},\ 0_{3\times1})\end{aligned} \tag{10}$$

Contrary to the yields, the risk price loads on both spanned and hidden factors. However, the loadings of r_t^* and π_t^* on the risk price exactly equal their marginal impacts on the expected X_{t+1} in equation (7). This restricts that the effects of r_t^* and π_t^* on the risk premium offset their effects on expected future short rates. Intuitively, since longer-term yields are the sum of expected future short rates and risk premiums, any variation in these hidden factors leaves yields unchanged under this restriction.

Given such a shadow rate and the risk-neutral (Q) process in equation (9) the bond prices are exponentially affine in factors X_t as given in equation (A.1), and the coefficients can be computed recursively as in (A.3) and (A.4) in Appendix A.

Since latent factors may be arbitrarily rotated (see Dai and Singleton (2000)), a set of parameter restrictions is necessary to normalize the latent factors. We employ the rotation in Joslin et al. (2011):

$$\delta_0 = 0 \quad \delta_1 = (1,\ 1,\ 1)' \quad \mu^Q = (k_\infty^Q,\ 0,\ 0)'$$

$$\Phi^Q = \begin{pmatrix} \lambda_1^Q & 0 & 0 \\ 0 & \lambda_2^Q & 0 \\ 0 & 0 & \lambda_3^Q \end{pmatrix}$$

Σ is lower triangular

where λ^Q s are real, distinct eigenvalues of Φ^Q and lie between 0 and 1.

A closed-form solution for the forward rate subject to the lower bound can be conveniently derived in this model under certain approximations. The corresponding yield curve can then be readily obtained from the term structure of the forward rates. We sketch the derivation, summarize the necessary approximations, and present the solution below; interested readers are referred to Appendix A for further details.

We work directly on the m-period-ahead shadow forward rate at time t ($f_{t,m}$):

$$f_{t,m} = (m+1)y_{t,m+1} - my_{t,m} \tag{11}$$

where $y_{t,m}$ is the yield of m-period maturity in the shadow rate DTSM. Under the risk-neutral measure, the shadow forward rate $f_{t,m}$ is the center of the distribution of the adjusted future shadow rate:

$$f_{t,m} = E_t^Q(\tilde{s}_{t+m}) \tag{12}$$

where $\tilde{s}_{t+m} = s_{t+m} - CAT_m$ and CAT_m is a time-invariant convexity adjustment term given in (A.6). Equation (A.9) in Appendix A also gives the conditional variance of $\tilde{s}_{t+m}$ (and s_{t+m}) denoted by σ_m^2.

However, when the short rate is subject to the ZLB, such a relationship is generally not expected to hold between the *actual* forward rate and the *actual* short rate because the short rate is no longer normally distributed:

$$\underline{f}_{t,m} \neq E_t^Q(i_{t+m}) - CAT_m \tag{13}$$

where $\underline{f}_{t,m}$ is the actual forward rate and $i_{t+m} = max(\underline{i}, s_{t+m})$ is the actual short rate. Instead, we show in Appendix A that approximations that are worked out in Wu and Xia (2016) are necessary to arrive at an analytical solution. To summarize these approximations,

we postulate that:

$$\underline{f}_{t,m} \approx E_t^Q(max(\underline{i}, s_{t+m})) - \widetilde{CAT}_{t,m} \tag{14}$$

where $\widetilde{CAT}_{t,m}$ reflects the convexity adjustment term for i_{t+m}, which becomes the time-invariant convexity adjustment term CAT_m if i_{t+m} is completely Gaussian. The following approximation holds.

$$\underline{f}_{t,m} \approx E_t^Q(max(\underline{i}, \tilde{s}_{t+m})) \tag{15}$$

given the following requirement for term $\widetilde{CAT}_{t,m}$:

$$\widetilde{CAT}_{t,m} = \sigma_m g\left[\frac{(f_{t,m} - (\underline{i} - CAT_m))}{\sigma_m}\right] - \sigma_m g\left[\frac{f_{t,m} - \underline{i}}{\sigma_m}\right] \tag{16}$$

where the functions $g(x) = x \cdot \mathbf{\Phi}(x) + \phi(x)$ and $\mathbf{\Phi}(\cdot)$ and $\phi(\cdot)$ are the cumulative distribution function and probability density function of the standard normal distribution, respectively. Note that when the short rate is far above the lower bound, we have $\mathbf{\Phi}(\cdot) \to 1$ and $\phi(\cdot) \to 0$ in the limit, that is, when $\widetilde{CAT}_{t,m}$ becomes exactly CAT_m.

Using equation (A.11) and the conditional distribution of $\tilde{s}_{t+m}$ under the risk-neutral measure, an analytical solution to the actual forward rate is:

$$\begin{aligned}\underline{f}_{t,m} &= \underline{i} + \sigma_m\left[\frac{(f_{t,m} - \underline{i})}{\sigma_m} \cdot \mathbf{\Phi}\left(\frac{f_{t,m} - \underline{i}}{\sigma_m}\right) + \boldsymbol{\phi}\left(\frac{f_{t,m} - \underline{i}}{\sigma_m}\right)\right] \\ &= \underline{i} + \sigma_m \cdot g\left(\frac{f_{t,m} - \underline{i}}{\sigma_m}\right)\end{aligned} \tag{17}$$

where,

$$f_{t,m} = \delta_1' \left(\sum_{j=0}^{m-1} (\Phi^Q)^j \right) \mu^Q + \delta_0 + \delta_1' (\Phi^Q)^m \cdot X_t - CAT_m \tag{18}$$

$$\sigma_m^2 = \delta_1' \left(\sum_{j=0}^{m-1} (\Phi^Q)^j \Sigma\Sigma' (\Phi^{Q'})^j \right) \delta_1 \tag{19}$$

2.2 Inflation Dynamics

We employ a standard trend-cycle decomposition model, akin to those in Del Negro et al. (2017) and Johannsen and Mertens (2021), to extract inflation trend.

$$\pi_t = \pi_t^* + \pi_t^c \tag{20}$$

$$\pi_t^* = \pi_{t-1}^* + \eta_{\pi t} \tag{21}$$

$$\pi_t^c = \phi_1 \pi_{t-1}^c + \phi_2 \pi_{t-2}^c + \epsilon_{\pi t}^c \qquad \epsilon_{\pi t}^c \overset{iid}{\sim} N(0, \sigma_{\pi c}^2) \tag{22}$$

where π_t is inflation rate. π_t^c is the cyclical component that is governed by a stationary AR(2) process.

To bring more information to bear on identifying inflation trend, we also include the information of long-run inflation expectation in the model. Specifically, we obtain data on the long-run inflation expectation π_t^s and assume it consists of inflation trend, π_t^*, and a temporary disturbance term, $\epsilon_{\pi t}^s$:

$$\pi_t^s = \pi_t^* + \epsilon_{\pi t}^s \quad \epsilon_{\pi t}^s \overset{iid}{\sim} N(0, \sigma_{\pi s}^2) \tag{23}$$

We follow Bauer and Rudebusch (2020) and use the Federal Reserve's perceived target rate (PTR) as a proxy for π_t^s for the U.S.. In the U.K., inflation targeting was adopted by the Bank of England in October 1992, but an explicit target rate was not established until 1998

(e.g., Mishkin and Posen (1998)). Consequently, we treat the inflation targets of the U.K. before 1998 as missing observations and set it to its explicit inflation target, which is 2.5% between 1998 and 2003 and 2% since 2004. Similarly, Bundesbank started to implement many features of an inflation-targeting regime in the 1970s, as pointed out in Bernanke and Mihov (1997). Therefore, we employ the inflation target derived in Bernanke and Mihov (1997) for π_t^s for Germany between 1975 and 1998, and then switch to 2%, around which the ECB sets its inflation target starting in 1999.

3 Data

We apply our model to three representative countries—the United States, the United Kingdom, and Germany—to extract real interest rate trends. For the U.S. and Germany, forward rates for maturities of 3 months, 6 months, and 12-120 months in 12-month intervals are constructed from the Federal Reserve Board's dataset and Bundesbank's website respectively, using the approach in Gürkaynak et al. (2007) [4]. For the U.K., the forward rates cover maturities between 1 and 10 years and are obtained from the Bank of England's database. The U.K. forward rates with maturities of less than one year are discarded because they are not consistently available and are contaminated by severe liquidity issues. The U.S. inflation rate is computed using the core PCE price index. The U.K. and German inflation rates are constructed using the core CPI obtained from the OECD database. The PTR data is retrieved from the Federal Reserve Board website. The sample for the U.S. spans October 1971 to April 2022. The dataset for Germany ranges from October 1972, when German yield data started to be available, to March 2022. The U.K. date date from January 1983 to March 2022. We dropped the data before 1983 because of the abnormally high inflation in

[4]We do not use 3-month yields directly, instead we utilize 3-month forward rates, avoiding the potential problem for the short end of yield curve constructed from their approach.

the U.K. during the 1970s[5].

The effective lower bound $\underline{i}$ is set to zero for the U.S. because the actual short rate in the U.S. has never dropped below zero [6]. The effective lower bound for the U.K. is also fixed to zero, as suggested by Andreasen and Meldrum (2015). For Germany, we adopt a time-varying effective lower bound following Kortela (2016). Before June 2016, the lower bound for Germany is set to zero, because the ECB's deposit rate was positive. Since then, the ECB has begun experimenting with negative interest rates. As a result, from June 2016 to the end of our sample period, we rely on the release of new ECB deposit rates to divide the sample into several intervals. In each subsample, the lower bound is set as the minimum of ECB deposit rate and observed forward rates.

4 Estimation

A state-space representation of our shadow rate unspanned DTSM can be written as

$$\begin{pmatrix} f_t^o \\ \pi_t \\ \pi_t^s \end{pmatrix} = \bar{\boldsymbol{H}}_t(Z_t) + \begin{pmatrix} e_t \\ 0 \\ \epsilon_{\pi t}^s \end{pmatrix} \quad e_t \overset{iid}{\sim} N(0, R) \tag{24}$$

$$Z_t = \tilde{\boldsymbol{\mu}} + \boldsymbol{F} Z_{t-1} + \tilde{\boldsymbol{v}}_t \quad \tilde{\boldsymbol{v}}_t \overset{iid}{\sim} N(0, Q) \tag{25}$$

where f_t^o is an $n \times 1$ vector containing n observed forward rates at time t, and the vector $Z_t = (X_{1t}, X_{2t}, X_{3t}, r_t^*, \pi_t^*, \pi_t^c, \pi_{t-1}^c)'$ stores all latent factors. e_t represents $i.i.d.$ measurement errors with a diagonal variance-covariance matrix R.[7] $\tilde{\boldsymbol{v}}_t = (u_t', \eta_{rt}, \eta_{\pi t}, \epsilon_{\pi t}^c, 0)'$. The parameters

[5] All empirical results remain qualitatively similar if this period in the U.K. is included and those results are available upon request.

[6] Our empirical results are robust to altering $\underline{i}$ to 0.25 which is adopted as the effective lower bound in Wu and Xia (2016).

[7] We follow Joslin et al. (2011) and Bauer and Rudebusch (2020) to posit an identical variance to measurement errors of various maturities.

have the following forms:

$$\tilde{\boldsymbol{\mu}} = \begin{pmatrix} (I_3 - \Phi)\bar{X} \\ 0 \\ 0 \\ 0 \\ 0 \end{pmatrix} \qquad \boldsymbol{F} = \begin{pmatrix} \Phi & (I_3 - \Phi)\gamma & (I_3 - \Phi)\gamma & 0 & 0 \\ 0_{1\times 3} & 1 & 0 & 0 & 0 \\ 0_{1\times 3} & 0 & 1 & 0 & 0 \\ 0_{1\times 3} & 0 & 0 & \phi_1 & \phi_2 \\ 0_{1\times 3} & 0 & 0 & 1 & 0 \end{pmatrix}$$

$$R = \sigma_e^2 I_n \qquad Q = \begin{pmatrix} \Sigma\Sigma' & \gamma\sigma_{\eta r}^2 & \gamma\sigma_{\eta\pi}^2 & 0 & 0 \\ \gamma'\sigma_{\eta r}^2 & \sigma_{\eta r}^2 & 0 & 0 & 0 \\ \gamma'\sigma_{\eta\pi}^2 & 0 & \sigma_{\eta\pi}^2 & 0 & 0 \\ 0 & 0 & 0 & \sigma_{\pi c}^2 & 0 \\ 0 & 0 & 0 & 0 & 0 \end{pmatrix}$$

The specific representation of $\bar{\boldsymbol{H}}_t(Z_t)$ is

$$\bar{\boldsymbol{H}}_t(Z_t) = \begin{pmatrix} H_t(X_{1t}, X_{2t}, X_{3t}), & \pi_t^* + \pi_t^c, & \pi_t^* \end{pmatrix}'$$

where $H_t(\cdot)$ is a nonlinear function approximating the forward rates of various maturities when the short rate is subject to an effective lower bound, according to equation (17).

Because the measurement equation (24) is nonlinear in the state variables owing to the approximation function $H_t(\cdot)$, the Kalman filter cannot be applied directly. Therefore, we employ the extended Kalman filter (EKF) based on a linear expansion of the nonlinear function to predict and update the state variables.

Denote by $H_t(X_{t|t-1})$ the estimate of $H_t(X_t)$ using information up to time $t-1$. Let the $3 \times n$ matrix $\tilde{H}_t$ be the first-order derivative of the nonlinear function $H_t(X_t)$ with respect

to X_t evaluated at $X_{t|t-1}$. Specifically,

$$\tilde{H}_{mt} = \left(\frac{\partial H_{mt}(X_{t|t-1})}{\partial X_{1t}}\bigg|_{X_{t|t-1}} \quad \frac{\partial H_{mt}(X_{t|t-1})}{\partial X_{2t}}\bigg|_{X_{t|t-1}} \quad \frac{\partial H_{mt}(X_{t|t-1})}{\partial X_{3t}}\bigg|_{X_{t|t-1}} \right)' \tag{26}$$

Each column of $\tilde{H}_t$, $\tilde{H}_{mt}$ stacks the first-order derivatives of the m-period forward rate with respect to the state variable X_t given information up to time $t-1$. $\tilde{H}_{mt}$ is given by $\tilde{H}_{mt} = \mathbf{\Phi}\left(\frac{\tilde{A}_m + \tilde{B}_m' X_{t|t-1} - i}{\sigma_m}\right) \times \tilde{B}_m$, where $\tilde{A}_m$, $\tilde{B}_m$, and σ_m are computed for different maturities m, according to (A.5) and (A.9). The updating of the state variables proceeds as follows.

$$K_t = V_{t|t-1}\tilde{H}_t(\tilde{H}_t' V_{t|t-1}\tilde{H}_t + R)^{-1} \tag{27}$$

$$X_{t|t} = X_{t|t-1} + K_t(f_t^o - H_t') \tag{28}$$

$$V_{t|t} = (I_3 - K_t\tilde{H}_t')V_{t|t-1} \tag{29}$$

$$V_{t|t-1} = FV_{t-1|t-1}F' + Q \tag{30}$$

Meanwhile, the part of inflation decomposition in the measurement equation is linear in state variables, and thus, the standard Kalman filter can be applied directly to update and predict related state variables.

In total, we have 30 parameters to estimate: three in Φ^Q, k_∞^Q; six in Σ; nine in Φ; four standard deviations of innovations to r_t^*, π_t^*, π_t^c, and π_t^s, σ_e, ϕ_1 and ϕ_2; and four free parameters in $\bar{X}$ and γ. To better account for estimation uncertainty, we employ the MCMC estimation algorithm similar to that in Bauer and Rudebusch (2020) to simulate the posterior distribution of state variables and model parameters. The log-likelihood function of our model is composed of three components, which we label as the Q-likelihood and P-likelihood regarding forward rates and the π-likelihood involving inflation rate. The Q-likelihood measures the cross-section fitting of the forward rate curve, whereas the P-likelihood pertains

to the dynamics of all state variables. We compute the π-likelihood from the trend-cycle decomposition of the inflation rate in equations (20) through (23). Each component involves different groups of parameters. The Q-likelihood is proportional to the measurement errors at any time t:

$$llkQ \propto -\frac{1}{2}|f_t^o - H_t'|/\sigma_e^2 \tag{31}$$

Consequently, it involves only the parameter set $(k_\infty^Q, \Phi^Q, \Sigma, \sigma_e)$. The P-likelihood at each period can be written as

$$llkP = -\frac{1}{2}(log|\Omega_v| + v_t'\Omega_v^{-1}v_t) \tag{32}$$

$$\Omega_v = \begin{pmatrix} \Sigma\Sigma' & (\sigma_{\eta r}^2 + \sigma_{\eta\pi}^2)\gamma \\ (\sigma_{\eta r}^2 + \sigma_{\eta\pi}^2)\gamma' & (\sigma_{\eta r}^2 + \sigma_{\eta\pi}^2) \end{pmatrix} \quad v_t = (u_t',\ (\eta_{rt} + \eta_{\pi t}))'$$

Therefore, P-likelihood is determined by $(\Sigma, \Phi, \bar{X}, \gamma, \sigma_{\eta r}^2, \sigma_{\eta\pi}^2)$. Similarly, π-likelihood depends on $(\phi_1, \phi_2, \sigma_{\eta\pi}^2, \sigma_{\pi c}^2, \sigma_{\pi s}^2)$.

Our approach employs a block-wise Bayesian estimation that combines the Metropolis-Hastings (M-H) sampler and Gibbs sampler. First, given parameter draws, state variables are simulated using a smoother, as outlined in Kim and Nelson (1999). Conditional on state variables, parameters are drawn block by block. The parameters are divided into 10 blocks: (1) (k^Q, Φ^Q), (2) Σ, (3) $(\gamma, \bar{X})$, (4) $\sigma_{\eta r}^2$, (5) Φ, (6) σ_e^2, (7) (ϕ_1, ϕ_2), (8) $\sigma_{\eta\pi}^2$, (9) $\sigma_{\pi c}^2$, and (10) $\sigma_{\pi s}^2$. The parameters in block (1) only affect the Q-likelihood, whereas those in blocks (3) and (4) affect P-likelihood. Σ in block (2) is related to both Q- and P-likelihoods. The parameters in blocks (7)-(10) determine the π-likelihood.

Following Chib and Greenberg (1995), we apply the block-wise M-H algorithm to blocks (1)-(4). In each block, we optimize the log-likelihood functions over the parameters in the block, conditional on all other parameters and state variables. Then, we use the resulting

mode and Hessian matrix to construct independence proposal distributions, similar to Chib and Ergashev (2009). The proposal distribution is a multivariate t-distributions with five degrees of freedom. For blocks (5) and (6), Φ and σ_e^2 are parameters in the linear equations, where the posterior distribution of parameters are known functions of prior and data. Therefore, the Gibbs sampling method is employed to simulate draws for Φ and σ_e^2. Similarly, the conditional posterior distribution of parameters in blocks (7)-(10) can also be obtained using the Gibbs sampler. Once all the parameters are drawn, we move to the next iteration to stimulate state variables conditional on parameter draws.

The priors of the parameters for each country is described in Appendix B. The starting values of the simulation are obtained by maximizing the joint log-likelihood function through the classical estimation. All parameters have the same type of prior distribution but with different means and tightnesses in different countries. We set the number of simulations to 100,000 and use the second half of the draws to construct the posterior distribution of the state variables and parameters[8].

5 Empirical Results

5.1 Estimates of the Real Interest Rate Trend

Figure 1 reports our estimates of the shadow rates with 90%-confidence intervals for the U.S. (top panel), the U.K. (middle panel), and Germany (bottom panel)[9]. Note that when the short rate is far above its effective lower bound, prior to roughly 2010, the shadow

[8]There are related papers where parameters are time-varying over the zero lower bound period, such as Kulish et al. (2017), Mavroeidis (2021), and Aruoba et al. (2022). We re-estimate our SDTSM using a subsample till the end of 2017 for a robustness check. The estimates from the subsample do not change substantially compared to the full-sample estimates.

[9]All other figures showing estimates separately for the three countries are also organized in this particular order.

rate estimate coincides with the short rate estimate[10]; during this period, the uncertainty around the shadow rate estimates is considerably smaller than that during the ZLB period after 2010, consistent with intuition. In the U.S., the shadow rate started rising in the middle of the 1970s and reached a peak in the first half of the 1980s. Starting in the mid-80s, the shadow rate in the U.S. declined persistently following a downward trend and fell persistently below zero, the effective lower bound, at the beginning of 2009. Since then, the shadow rate continued to drift downward in the negative region until the end of 2011, when it was elevated for a short period of time, approaching zero by the end of 2012. Since then, it has resumed declining and reached a bottom around 2014 before starting to climb up again until the first half of 2019. The shadow rate quickly fell below zero at the onset of the COVID pandemic and remained in the negative regime for two years. The shadow rate has risen above zero since 2022, as the Fed suddenly started to tighten its monetary policy. Our shadow rate estimates share a broadly similar pattern to those of Wu and Xia (2016). However, our estimates are noticeably more variable and more negative at the bottom, reflecting the drifting trend embedded in our model [11].

In the U.K., the shadow rate started to decline persistently since the beginning of the 1990s, and similar to the U.S., its decline was further accelerated by the GFC when the U.K. shadow rate also dropped below zero persistently in 2009 and remained negative until the end of 2017. The shadow rate in the U.K. remained positive since 2018 but also turned negative during the COVID pandemic. Earlier than its counterpart in the U.S., the shadow rate in the U.K. bounced back to positive at the end of 2021 and continued to rise afterwards. Again, our estimates of the U.K. shadow rate are similar to those using the methods of Wu and Xia (2016), Wu and Xia (2017), and Wu and Xia (2020)[12]. The shadow rate in Germany

[10]Note that the short rate is assumed to be latent, as standard in the DTSM literature, which explains the estimation uncertainty.

[11]The cointegrating vectors are reported in Table A1.

[12]Their U.K. shadow rate estimates are published on their website https://sites.google.com/view/jingcynthiawu/shadow-rates?authuser=0.

experienced some fluctuations in the 70s and 80s and did not start a persistent decline until around the mid-90s. It fell below zero in the second half of 2009 but quickly turned positive in 2010. It then dropped below zero again around the end of 2011 and remained negative until the end of our sample, except for 2014 and the first month of 2015 [13].

Figure A1 plots our shadow rate estimates together and shows the co-movement among shadow rates in the three countries. All shadow rates have been declining persistently in recent decades. Despite a slightly different starting time, the shadow rates all share a similar downward trend since the mid-90s and all shadow rates fell below zero following the GFC. The U.S. shadow rate experienced the largest decline and the lowest bottom in the wake of the GFC. However, it also embraced the strongest comeback and stayed above the ZLB for the longest period before the COVID pandemic (from the end of 2016 to the end of 2020), whereas the U.K. shadow rate remained positive for a shorter period between 2018 and 2020. During the COVID pandemic, the shadow rates in the U.S. and U.K. fell below zero again. They both declined to around -3% and returned to positive territory at the beginning of 2022 and the end of 2021, respectively. On the other hand, the German shadow rate was stuck in the negative region for almost the entire post-GFC period.

Figure 2 presents our real interest rate trend estimates with the 90% confidence bands for the three countries. For the U.S. and Germany, the real interest rate trends appear to have an upward trend in the 1970s and the 1980s, respectively, before they started to decline in the mid-80s for the U.S. and the mid-90s for Germany. The U.K. real interest rate trend reached a plateau in the 1980s and then dropped to a low level around 1990. Although it climbed to around 10% in the early 90s the real interest rate trend has declined persistently since then. This figure also reveals that the real interest rate trends in all three countries fell below zero and stayed in the negative territory in the wake of the GFC. To facilitate

[13] Although a Euro shadow rate is also published on Wu and Xia's website it is based on a different set of interest rates using a substantially different sample period and thereby we do not attempt to make a comparison.

a cross-country comparison, Figure A2 plots three real interest rate trends in one figure. Visually, the three real interest rate trends all share a pattern of persistent decline starting from the mid-90s. This notable declining trend began well before the GFC, but the GFC undoubtedly accelerated this trend. Recall that the real interest rate trend is defined as the long-run forecast of the shadow rate (in real term). Therefore, the real interest rate trends move more smoothly than the shadow rates do. For example, although the U.S. shadow rate dropped below zero in 2008, its real interest rate trend did not drop below zero until the beginning of 2015. On the other hand, this also reflects a very aggressive U.S. monetary policy easing at the time to cope with the unprecedented financial crisis. The German real interest rate trend was the first to consistently fall below zero around the middle of 2014, whereas the U.K. interest rate trend did not fall below zero until the end of 2014.

Even if the magnitudes of the declines differ among the real interest rate trends, a similar trajectory is evident. We follow the empirical approach of Holston et al. (2017) to study the co-movement among the three real interest rate trends. We first perform the augmented Dickey-Fuller test for real interest rate trends, and the results in Panel A of Table A2 confirm that they all have a unit root. We then choose the real interest rate trends between January 1991 and March 2022 and employ the Johansen cointegration test for three real interest rate trends. The results are presented in Panel B of Table A2. The cointegration test suggests two cointegrating vectors and one common stochastic trend for three real interest rate trends. In light of these results, we estimate a VECM model with 24 lags; the error-correction estimates are reported in Panel C of Table A2. Based on the VECM model, we implement a variance decomposition using Cholesky factorization with the ordering of the U.K., Germany, and the U.S.. The decomposition results are shown in Figure 3. The decomposition results indicate clear interdependence among the three real interest rate trends. For instance, shocks to the US real interest rate trend contribute greatly to variations in German and UK real interest rate trends, and the longer the horizon, the larger the contributions. To check the robustness

of the results, we also employ a different ordering and report the variance decomposition results using the ordering of Germany, the U.K., and the U.S. in Figure A4. Although the numerical results somewhat change, the co-movement and interdependence among the three real interest rate trends remain robust. These results lead us to draw a conclusion similar to Holston et al. (2017) that whatever forces behind the declining real interest rate trends must have had cross-country impacts.

5.2 Forecast of Shadow Rate and Zero Lower Bound Probabilities

Since the trajectory of the shadow rate and probability of a binding ZLB is of great interest to policymakers and market participants, we take the U.S. as an example to illustrate how our model works to deliver these estimates. According to equations (8) and (25), we forecast h-month-ahead shadow rate at time t:

$$\begin{aligned} s_{t+h|t} &= E_t(s_{t+h}) \\ &= \delta_0 + \delta_1' E_t(X_{t+h}) \\ &= \delta_0 + \delta_1' \left[(I_3 - \Phi) \sum_{k=0}^{h-1} \Phi^k \bar{X} + \Phi^h X_t + (I_3 - \Phi) \sum_{k=0}^{h-1} \Phi^k \gamma (r_t^* + \pi_t^*) \right] \end{aligned} \tag{33}$$

We employ 50,000 sets of estimated parameters and latent factors in MCMC to compute the distribution of the rate forecast. Figure 4 plots the median of h-month-ahead forecasts of the shadow rate, s_{t+h}, at time t with 90%-confidence intervals. The horizons are 1, 3, 6, 12, and 24 months. Our model suggests that at the end of our sample period (April 2022), the short rate is forecasted to continue to rise and stay above the ZLB at all horizons.

It is worth noting that the shadow rate we forecast contains a slow-moving trend by construction and needs enough sample to build its movement. Beside, our forecasts of shadow rate reflect the belief of the market on future short rate, which may be at odds with

what the FOMC signals. For example, in early 2012 the FOMC committed to keep zero interest rate through to late 2014. However, our 24-month forecast of shadow rate implies that in 2012 the market expected the rate to rise in the middle of 2014 earlier than the date the FOMC indicated.

Next, we compute the probability of a binding ZLB for different horizons at each time point. Specifically, the h-horizon-ahead expected shadow rate at time t is laid out in equation (33). Based on equation (25), we define the variance-covariance matrix of $[u_t \ \eta_{rt} \ \eta_{\pi t}]'$ as Ω_v, and the conditional variance of the forecasted shadow rate can be expressed as

$$Var_t(s_{t+h}) = \Omega_v + \Phi\Omega_v\Phi' + (\Phi^2)\Omega_v(\Phi^2)' + \cdots + (\Phi^{h-1})\Omega_v(\Phi^{h-1})' \tag{34}$$

Because the Gaussian feature is maintained in our model, we can compute the probability of $s_{t+h} < 0$ given $E_t(s_{t+h})$ and $Var_t(s_{t+h})$.

Again, we rely on the same set of 50,000 MCMC draws to compute the estimate and confidence interval of this probability. The results are shown in Figure 5. In the panel of h-Month Forecast Probability, at each time point t we show the median probability that the ZLB binds at $t + h$ and its 90%-confidence interval. A few points are worth noting. First, in each panel, the probability of a binding ZLB is almost negligible before 2008, with the exception of a few months in the early 2000s. Second, the probability starts to rise at the end of 2008 and remains at a very high level until the middle of 2011, when the Fed finished its second round of quantitative easing (QE) and the probability takes a downturn. The probability of a binding ZLB starts to climb in the second quarter of 2012, when the Fed launched QE3 in September of that year. This probability reaches and remains at a high level in 2014, and then starts to decline as the Fed halted its bond purchase at the end of 2014. Notably, Fed Chairman Bernanke, in May 2013, surprised the market by mentioning a potential taper. Although the probability rises during 2013 in our forecasts, there is an

evident drop around that time point, reflecting the impact of Bernanke's speech. Later, the forecast probability experiences another slide around October when the Fed officially announced its plan to taper. Third, at all horizons, the probability spikes again at the onset of the pandemic in 2020. However, it starts to decline persistently around October 2021 before the Fed officially announced to taper bond purchase in November in response to increasing inflation, which points to the market participants' expectation of higher policy rates as the Fed attempts to contain rising inflation. These results show that our model generates useful forecasts of the shadow rate and the probability of a binding ZLB that seem consistent with major macroeconomic events and policy announcements.

5.3 Out-of-sample Forecasts

Joslin et al. (2011) show that the no-arbitrage restrictions are irrelevant to forecast the pricing factors in an affine and Gaussian term structure model. However, we are interested in whether our model, which becomes nonlinear due to the ZLB constraint, can improve the yields forecast upon most existing affine models by imposing the no-arbitrage restrictions and explicitly accounting for the ZLB constraint. This exercise is interesting in its own right as it can shed light on the aspects of the DTSM that we need to further work on. To this end, we conduct out-of-sample forecast exercises to compare the performance of our model and several existing models. For each country, we forecast the ten-year forward rate using four different models: the random walk (RW) model, the standard DTSM in Joslin et al. (2011), DTSM with drifting trends as in Bauer and Rudebusch (2020) (BR), and our shadow rate DTSM with drifting trends (SDTSM). The RW model assumes a driftless random-walk process for forward rates. The DTSM has three stationary factors, which are the first three principal components of yields. We focus on the forecasting horizons of 6, 10, 20, 30, and 40 months, and the forecasts start once 20 observations are available. In each period, all data

up to that date are used to estimate the model and then make forecasts[14].

Table 1 shows the results of this study. In each panel, the root mean squared errors (RMSEs) are shown in the first three rows. To compare forecasts from different models, we apply the Diebold Mariano (DM) test using RMSE as the evaluation metric against the null hypothesis that forecasts from our SDTSM are not more accurate than the benchmark model. The associated p-values reported in the last two rows of each panel are adjusted to improve the small-sample performance following Harvey et al. (1997). These results show that our SDTSM can yield better forecasts than DTSM for almost all three countries and all horizons, except for three long horizons in the U.K. and the 30-month horizon in Germany. Furthermore, the improvement is statistically significant at short horizons for the U.S. and Germany. Compared to RW, the RMSEs from our SDTSM are close to those from RW, and the improvement is not significant. The results above suggest that adopting the shadow rate and drifting trends into an otherwise standard DTSM can significantly improve interest rate forecasts.

To compare the forecast results of our SDTSM with those of BR, we conduct a quarterly out-of-sample forecast for the U.S. forward rate spanning from 1977Q3 to 2018Q1, which is identical to the sample period in Table 5 of BR[15]. The last forecast is made during the first quarter of 2008. In our model, the forecast is conducted in the last month of each quarter and we take the average of three monthly forward rates in each quarter as the corresponding quarterly forward rate. For the BR forecast, we adopt their estimated shifting endpoint model by pre-estimating parameters using full-sample data, but only using information up to each forecast date to generate state variables and make forecasts. The results are shown in the lower part of Panel A of Table 1. We choose the same forecasting horizons that cover

[14]We do not re-estimate the SDTSM in each period because of the very high computational cost. Instead we use the parameter estimates from 5.1 and then use data available up to each forecast date to extract the latent factors and forecast forward rates.

[15]The BR model relies on PTR and external estimates of natural rate that are quarterly. Thus we compare quarterly forecasts.

4 through 40 quarters. Our SDTSM yields lower RMSEs than the BR model at all horizons, and the improvement is statistically significant at the 4-quarter horizon. These results seem to suggest that introducing a shadow rate to account for the ZLB helps further improve the forecast accuracy of the yield curve upon adding persistent interest trends.

5.4 Term Premium and Inflation Uncertainty

We follow Wright (2011) and investigate the relationship between term premium and inflation uncertainty as an important diagnostic check of our model. As noted in the previous sections, our model device essentially summarizes the economic condition embodied in the entire yield curve with a single series of the shadow rate and relies on its long-run forecast to reflect the dynamics of the real interest rate trend. As such, the key to this successful transformation is a sensible term premium estimate. Intuitively, the term premium is defined as the difference between the long-term yields and expectations of future short rates. Past literature employing standard DTSM without drifting trends mostly attributes the high persistence of yields to the term premium. As illustrated in Kim and Orphanides (2012) and Bauer and Rudebusch (2020), models such as ours can produce more stationary term premium estimates by allowing persistent dynamics for the short (shadow) rate. In addition, by explicitly accounting for the ZLB, the shadow rate in our model is allowed to drift even further than the short rate in a standard Gaussian DTSM, helping produce an even more stable term premium estimate.

Figure 6 reports the estimated term premium of the ten-year yield with 90%-confidence intervals as a representative term premium for all three countries[16]. The estimated term premiums all appear stationary, and the Augmented Dickey-Fuller (ADF) test rejects the null and confirms stationarity. A cursory glance at Figure A5 suggests some co-movements

[16]We refer interested readers to Appendix C for details on the technical derivations of the term premium in our model.

among the term premia in the three countries. To investigate this issue, we apply the Principal Component Analysis (PCA) to the three term premia. The results in Panel A of Table A3 show that the first principal component can account for approximately 66% of the total variations. To investigate the extent to which each term premium is exposed to this common factor, we regress each of the three term premiums on the first PC and present the results in Panel B of Table A3. The $adj.R^2$ for the U.S. term premium is as high as 91% indicating that this first PC originates primarily from the U.S. term premium.

Past literature has built relationships between the term premium and inflation. For example, Rudebusch and Swanson (2008) show the role of inflation in the fitting term premium in a DSGE model. Wright (2011) works on yields and inflation in ten countries and finds that inflation uncertainty is able to explain term premium movement. As he elaborates on the paper intuitively, an increasing inflation uncertainty in principle makes long-term bonds riskier and thus raises the term premium. We attempt to investigate whether such a relationship exists for a more stationary term premium estimate from our model. We first construct an inflation uncertainty measure following Stock and Watson (2007) and Wright (2011). Specifically, we use the unobserved component stochastic volatility (UCSV) model to decompose the inflation rate π_t for each country into a stochastic trend τ_t^{π} and transitory shock η_t,

$$\pi_t = \tau_t^{\pi} + \eta_t \quad \eta_t \overset{iid}{\sim} N(0, \xi_{\eta t}^2) \tag{35}$$

$$\tau_t^{\pi} = \tau_{t-1}^{\pi} + \epsilon_{\tau t} \quad \epsilon_{\tau t} \overset{iid}{\sim} N(0, \xi_{\tau t}^2) \tag{36}$$

$$log\xi_{\eta t}^2 = log\xi_{\eta t-1}^2 + v_{\eta t} \tag{37}$$

$$log\xi_{\tau t}^2 = log\xi_{\tau t-1}^2 + v_{\tau t} \tag{38}$$

where $(v_{\eta t},\ v_{\tau t})$ follow an i.i.d $\mathbf{N}(0, I_2)$. Because the term premium estimates for the U.K. start from January 1983, we focus on inflation uncertainty and the term premium since

then. The UCSV model is applied to the monthly inflation rate in each country and is estimated using the MCMC method proposed by Stock and Watson (2007). We select the estimated standard deviation of the permanent shock as a measure of inflation uncertainty, as in Wright (2011). The standard deviation of the permanent shock to the inflation rate for each economy is displayed in Figure A6. The inflation uncertainty measure was large in the early 2000s for the U.S. and the 1990s for Germany. There was a hike in the measures taken in all three countries at the beginning of the COVID pandemic.

With each country's inflation uncertainty measure, we run a panel regression with the fixed effect of the term premium on the inflation uncertainty measure as follows:

$$TP_{it} = a_i + b \cdot INF_{it} + \epsilon_{it} \tag{39}$$

where TP_{it} is the term premium for country i at time t, a_i accounts for country-specific fixed effect, and INF_{it} denotes the inflation uncertainty measure. The results are reported in Table 2. The corresponding p-values are obtained using block bootstrap, where the original data is divided into blocks consisting of six observations. In each bootstrapped sample, we reconstruct a set of term premiums and inflation uncertainty using blocks of six months' original data under the null hypothesis, run the panel regression of equation (39), and compute the t-statistic of coefficient b. The number of bootstrap iterations is 50,000, and the last 25,000 iterations are kept to generate our bootstrapped distribution of the t-statistic. The estimate of coefficient b in the regression is positive and statistically significant. This result suggests that, on average, a higher term premium is associated with higher inflation uncertainty among these countries, strongly corroborating the findings of Wright (2011)[17].

[17]We also use the survey measure of inflation uncertainty in Wright (2011) to carry out the same exercises. The results are contained in Appendix D.

5.5 Excess Return and Risk Factors

Cochrane and Piazzesi (2005) showed that the realized U.S. excess returns across various maturities can be forecasted by a single risk factor which is tent-shaped and a linear function of forward rates. To check whether our shadow rate DTSM with drifting trends can generate such risk factor dynamics, we use our estimated parameters and latent factors to analyze the relationship between excess returns and forward rates.

Specifically, with each of the 50,000 simulated sets of parameter estimates and state variables for the U.S., we compute the forward rates of different maturities using equation (17) and add the simulated innovation term $\hat{e}_t$ to obtain our simulated forward rates, $\hat{f}^s_{t,m}$. The simulated yields $\hat{y}^s_{t,m}$ are then computed using the simulated forward rates. As a result, we construct a group of $\{\hat{f}^s_{t,m},\ \hat{y}^s_{t,m}\}$ for maturities ranging from one month to ten years spanning the entire sample period for the U.S.. Given the simulated monthly forward rates and yields, we calculate the annual excess return for a m-month bond bought at time t and sold at $t+12$:

$$rx^m_{t+12} = m\hat{y}^s_{t,m} - (m-12)\hat{y}^s_{t+12,m-12} - \hat{y}^s_{t,12} \tag{40}$$

where $\hat{y}^s_{t,m}$ is the simulated m-month yield at time t. Following Cochrane and Piazzesi (2005), we collect the excess returns of 24-, 36-, 48-, and 60-month U.S. treasury bonds over our sample period,$\{rx^{24}_t,\ rx^{36}_t,\ rx^{48}_t,\ rx^{60}_t\}$, and regress the time series of each excess return on a constant, 12-month yield, and four forward rates.

$$rx^m_{t+12} = b_0 + b_1\hat{y}^s_{t,12} + b_2\hat{f}^s_{t,12} + b_3\hat{f}^s_{t,24} + b_4\hat{f}^s_{t,36} + b_5\hat{f}^s_{t,48} \tag{41}$$

where $\hat{f}^s_{t,m}$ denotes the simulated m-month forward rate at time t. Because we have 50,000 groups of simulated yields and forward rates, equation (41) is run 50,000 times for each

excess return, rx_t^m. We then compute the mean of the parameter estimates for all m.

The results are shown in Figure 7. The median adjusted R^2 for these regressions fall between 0.1 and 0.15. In general, our plots corroborate the results shown in Figure 1 in Cochrane and Piazzesi (2005). The lines representing the parameters for different excess returns appear close to a tent shape, although notably, the loadings on longer maturity rates in our exercise do not decline as much. Similar to their study, excess returns with longer maturities tend to have larger loadings on forward rates than returns with shorter maturities. We conclude that our model captures the risk dynamics as reported in Cochrane and Piazzesi (2005).

6 Conclusion

We develop a shadow rate DTSM with drifting trends to extract the long-run forecast of the shadow rate (in real term) as the real interest rate trend. Although the shadow rate, based on which our real interest rate trend is estimated, is not an actual rate that the household and business faces or the Fed sets, it more accurately reflects the overall financial market condition during the ZLB period (Wu and Zhang (2019)). As such, our estimate of the real interest rate trend provides a useful measure to track the shifting economic equilibrium condition and serves as a benchmark against which monetary policy stances may be assessed and on which asset management strategies may be based.

By utilizing a convenient analytical solution to forward rates, we provide estimates of real interest rate trends for the United States, the United Kingdom, and Germany by exploring treasury yield data in these countries. We find that the real interest rate trend in all the three countries has declined persistently since the 1990s. Although our model remains agnostic about the driving forces behind the declining trends and our estimation relies on an entirely different set of information, we reach a conclusion similar to that of Holston et al. (2017)

that there appears to be a strong co-movement among the falling real interest rate trends in these three major advanced economies, suggesting an important role of global factors in shaping their dynamics.

As a diagnostic check of our model, we find that our term premium estimates are notably more stationary than, for example, those in Wright (2011), who assumes a mean-reverting yield curve. However, our term premium estimates remain significantly and positively correlated with inflation uncertainty measures, consistent with the major findings of Wright (2011). We also find that the risk factor dynamics simulated from our model share a similar pattern to that in Cochrane and Piazzesi (2005) so that a tent-shaped linear combination of forward rates helps forecast the excess bond holding period return. We deem these results to support our model device that primarily works with long rates during the ZLB period to disentangle the expectation movements of future short rates from term premium dynamics.

We employ our model to produce the time-varying probabilities of a binding ZLB. We find that the changes in probabilities align well with major monetary policy announcements. Through an extensive out-of-sample forecast exercise, we show that our model compares favorably with several existing term structure models in forecasting the yield curve. In particular, explicitly accounting for the ZLB via the shadow rate approach can further improve the yield curve forecast upon the BR model that contributes to the literature by incorporating a drifting interest rate trend into the DTSM.

References

Andreasen, M. M. and Meldrum, A. (2015). Market beliefs about the UK monetary policy lift-off horizon: a no-arbitrage shadow rate term structure model approach. *Bank of England Working Paper*, 541.

Aruoba, S. B., Mlikota, M., Schorfheide, F., and Villalvazo, S. (2022). Svars with occasionally-binding constraints. *Journal of Econometrics*, 231(2):477–499.

Barsky, R., Justiniano, A., and Melosi, L. (2014). The natural rate of interest and its usefulness for monetary policy. *American Economic Review*, 104(5):37–43.

Bauer, M. D. and Rudebusch, G. D. (2020). Interest rates under falling stars. *American Economic Review*, 110(5):1316–54.

Bauer, M. D., Rudebusch, G. D., and Wu, J. C. (2014). Term premia and inflation uncertainty: empirical evidence from an international panel dataset: comment. *American Economic Review*, 104(1):323–337.

Bernanke, B. S. and Mihov, I. (1997). What does the Bundesbank target? *European economic review*, 41(6):1025–1053.

Black, F. (1995). Interest rates as options. *the Journal of Finance*, 50(5):1371–1376.

Carvalho, C., Ferrero, A., and Nechio, F. (2016). Demographics and real interest rates: Inspecting the mechanism. *European Economic Review*, 88:208–226.

Chib, S. and Ergashev, B. (2009). Analysis of multifactor affine yield curve models. *Journal of the American Statistical Association*, 104(488):1324–1337.

Chib, S. and Greenberg, E. (1995). Understanding the metropolis-hastings algorithm. *The american statistician*, 49(4):327–335.

Christensen, J. H. and Rudebusch, G. D. (2019). A new normal for interest rates? evidence from inflation-indexed debt. *Review of Economics and Statistics*, 101(5):933–949.

Cieslak, A. and Povala, P. (2015). Expected returns in treasury bonds. *Review of Financial Studies*, 28:2859–2901.

Cochrane, J. H. and Piazzesi, M. (2005). Bond risk premia. *American economic review*, 95(1):138–160.

Coroneo, L., Giannone, D., and Modugno, M. (2016). Unspanned macroeconomic factors in the yield curve. *Journal of Business & Economic Statistics*, 34(3):472–485.

Dai, Q. and Singleton, K. J. (2000). Specification analysis of affine term structure models. *The journal of finance*, 55(5):1943–1978.

Del Negro, M., Giannone, D., Giannoni, M. P., and Tambalotti, A. (2017). Safety, liquidity, and the natural rate of interest. *Brookings Papers on Economic Activity*, 2017(1):235–316.

Diebold, F. X., Li, C., and Yue, V. Z. (2008). Global yield curve dynamics and interactions: A dynamic nelson-siegel approach. *Journal of Econometrics*, 146:351–363.

Duffee, G. R. (2011). Information in (and not in) the term structure. *The Review of Financial Studies*, 24(9):2895–2934.

Duffie, D. and Kan, R. (1996). A yield-factor model of interest rates. *Mathematical finance*, 6(4):379–406.

Favero, C. A., Gozluklu, A. E., and Yang, H. (2016). Demographics and the behavior of interest rates. *IMF Economic Review*, 64(4):732–776.

Gali, J. (2008). *Monetary Policy, Inflation, and the Business Cycle: An Introduction to the new Keynesian Framework*. Princeton University Press.

Gürkaynak, R. S., Sack, B., and Wright, J. H. (2007). The US treasury yield curve: 1961 to the present. *Journal of monetary Economics*, 54(8):2291–2304.

Hamilton, J. D., Harris, E. S., Hatzius, J., and West, K. D. (2016). The equilibrium real funds rate: Past, present, and future. *IMF Economic Review*, 64(4):660–707.

Harvey, D., Leybourne, S., and Newbold, P. (1997). Testing the equality of prediction mean squared errors. *International Journal of forecasting*, 13(2):281–291.

Holston, K., Laubach, T., and Williams, J. C. (2017). Measuring the natural rate of interest: International trends and determinants. *Journal of International Economics*, 108:S59–S75.

Johannsen, B. K. and Mertens, E. (2021). A time series model of interest rates with the effective lower bound. *Journal of Money, Credit and banking*, 53(5):1005–1046.

Joslin, S., Priebsch, M., and Singleton, K. J. (2014). Risk premiums in dynamic term structure models with unspanned macro risks. *Journal of Finance*, 69(3):1197–1233.

Joslin, S., Singleton, K. J., and Zhu, H. (2011). A new perspective on gaussian dynamic term structure models. *The Review of Financial Studies*, 24(3):926–970.

Kim, C.-J. and Nelson, C. R. (1999). State-space models with regime switching: classical and gibbs-sampling approaches with applications. *MIT Press Books*, 1.

Kim, D. H. and Orphanides, A. (2012). Term structure estimation with survey data on interest rate forecasts. *Journal of Financial and Quantitative Analysis*, pages 241–272.

Kortela, T. (2016). A shadow rate model with time-varying lower bound of interest rates. *Bank of Finland Research Discussion Paper*, (19).

Kozicki, S. and Tinsley, P. A. (2001). Shifting endpoints in the term structure of interest rates. *Journal of monetary Economics*, 47(3):613–652.

Krippner, L. (2015). *Zero lower bound term structure modeling: A practitioner's guide*. Springer.

Kulish, M., Morley, J., and Robinson, T. (2017). Estimating dsge models with zero interest rate policy. *Journal of Monetary Economics*, 88:35–49.

Laubach, T. and Williams, J. C. (2003). Measuring the natural rate of interest. *Review of Economics and Statistics*, 85(4):1063–1070.

Laubach, T. and Williams, J. C. (2016). Measuring the natural rate of interest redux. *Business Economics*, 51(2):57–67.

Lubik, T. A. and Matthes, C. (2015). Calculating the natural rate of interest: a comparison of two alternative approaches. *Economic Brief*, 15(10).

Lunsford, K. G. and West, K. D. (2019). Some evidence on secular drivers of US safe real rates. *American Economic Journal: Macroeconomics*, 11(4):113–39.

Mavroeidis, S. (2021). Identification at the zero lower bound. *Econometrica*, 89(6):2855–2885.

Mishkin, F. S. and Posen, A. (1998). Inflation targeting: lessons from four countries. *NBER Working Paper*, 6126.

Morley, J. C., Nelson, C. R., and Zivot, E. (2003). Why are the beveridge-nelson and unobserved-components decompositions of gdp so different? *Review of Economics and Statistics*, 85(2):225–243.

Orphanides, A. (2001). Monetary policy rules based on real-time data. *American Economic Review*, pages 964–985.

Orphanides, A. and van Norden, S. (2002). The unreliability of output-gap estimates in real time. *Review of Economics and Statistics*, pages 569–583.

Piazzesi, M. and Schneider, M. (2007). Equilibrium yield curves. *in Daron Acemoglu, Kenneth Rogoff, and Michael Woodford, NBER Macroeconomics Annual 2006*, pages 389–442.

Rudebusch, G. D. and Swanson, E. T. (2008). Examining the bond premium puzzle with a dsge model. *Journal of monetary Economics*, 55:S111–S126.

Stock, J. H. (1994). Unit roots, structural breaks and trends. *Handbook of econometrics*, 4:2739–2841.

Stock, J. H. and Watson, M. W. (1998). Median unbiased estimation of coefficient variance in a time-varying parameter model. *Journal of the American Statistical Association*, 93(441):349–358.

Stock, J. H. and Watson, M. W. (2007). Why has US inflation become harder to forecast? *Journal of Money, Credit and banking*, 39:3–33.

Summers, L. H. (2016). The age of secular stagnation: What it is and what to do about it. *Foreign affairs*, 95(2):2–9.

Watson, M. W. (1994). Vector autoregressions and cointegration. *Handbook of econometrics*, 4:2843–2915.

Williams, J. C. (2017). Safety, liquidity, and the natural rate of interest: comments and discussion. *Brookings Papers on Economic Activity*, pages 295–303.

Wright, J. H. (2011). Term premia and inflation uncertainty: Empirical evidence from an international panel dataset. *American Economic Review*, 101(4):1514–34.

Wu, J. C. (2017). Safety, liquidity, and the natural rate of interest: comments and discussion. *Brookings Papers on Economic Activity*, pages 303–310.

Wu, J. C. and Xia, F. D. (2016). Measuring the macroeconomic impact of monetary policy at the zero lower bound. *Journal of Money, Credit and Banking*, 48(2-3):253–291.

Wu, J. C. and Xia, F. D. (2017). Time-varying lower bound of interest rates in europe. *Chicago Booth Research Paper*, (17-06).

Wu, J. C. and Xia, F. D. (2020). Negative interest rate policy and the yield curve. *Journal of Applied Econometrics*, 35(6):653–672.

Wu, J. C. and Zhang, J. (2019). A shadow rate new keynesian model. *Journal of Economic Dynamics and Control*, 107:103728.

Table 1: **Out-of-sample forecasts for the ten-year forward rate**

	Horizon in months				
Panel A: U.S.	6	10	20	30	40
Random Walk (RW)	0.77	0.98	1.34	1.52	1.69
Standard DTSM (DTSM)	0.86	1.11	1.72	2.18	2.82
Shadow rate DTSM (SDTSM)	0.77	1.01	1.37	1.56	1.75
p-values: SDTSM≥RW	0.61	0.83	0.80	0.79	0.78
p-values: SDTSM≥DTSM	0.02	0.10	0.13	0.12	0.11
Quarterly forecast: 1977Q3-2018Q1	Horizon in quarters				
	4	10	20	30	40
DTSM with drifting trends (BR)	1.28	1.65	2.25	2.23	2.59
Shadow rate DTSM (SDTSM)	1.11	1.62	2.18	2.19	2.46
p-values: SDTSM≥BR	0.05	0.34	0.23	0.29	0.00

the table is continued on the next page

The standard DTSM has three stationary observed factors which are the first three principal components of yield data. The SDTSM method is our shadow rate DTSM with drifting trends. The BR is the shifting endpoint model in Bauer and Rudebusch (2020). The monthly forecast spans full sample while the quarterly forecast for the U.S. starts in 1977Q3 and ends in 2018Q1. In the upper part of Panel A, the first three rows report the root mean squared errors (RMSE) from different models. The last two rows report p-values of Diebold-Mariano test with the small sample adjustment of Harvey et al. (1997), against the null hypothesis that the SDTSM does not improve the forecast compared with RW, DTSM. The lower part of Panel A follows the same manner comparing SDTSM to BR.

Table 1 (ctd.)

	Horizon in months				
Panel B: U.K.	6	10	20	30	40
Random Walk (RW)	0.63	0.81	1.12	1.35	1.56
Standard DTSM (DTSM)	0.75	0.96	1.29	1.50	1.69
Shadow rate DTSM (SDTSM)	0.72	0.95	1.34	1.61	1.84
p-values: SDTSM≥RW	0.99	0.99	0.99	0.98	0.97
p-values: SDTSM≥DTSM	0.32	0.49	0.64	0.70	0.69
	Horizon in months				
Panel C: Germany	6	10	20	30	40
Random Walk (RW)	0.73	0.88	1.11	1.31	1.43
Standard DTSM (DTSM)	0.87	0.99	1.21	1.36	1.53
Shadow rate DTSM (SDTSM)	0.72	0.90	1.17	1.37	1.48
p-values: SDTSM≥RW	0.44	0.82	0.96	0.95	0.86
p-values: SDTSM≥DTSM	0.01	0.15	0.32	0.53	0.33

In Panel B and C, the first three rows report the root mean squared errors (RMSE) from different models. The last two rows in each panel report p-values of Diebold-Mariano test with the small sample adjustment of Harvey et al. (1997), against the null hypothesis that the SDTSM does not improve the forecast compared with RW or DTSM.

Table 2: **Panel Dataset of Term Premium and Inflation Uncertainty**

Regression of term premium on inflation uncertainty	
s.d. of permanent shock to inflation rate	
Estimate	1.60
p-value	(0.02)

The table shows the estimates of b in the regression of term premium on inflation uncertainty as in equation (39). The p-values in parenthesis are obtained from a block bootstrap.

Figure 1: **The shadow rates for US, UK, and GM**

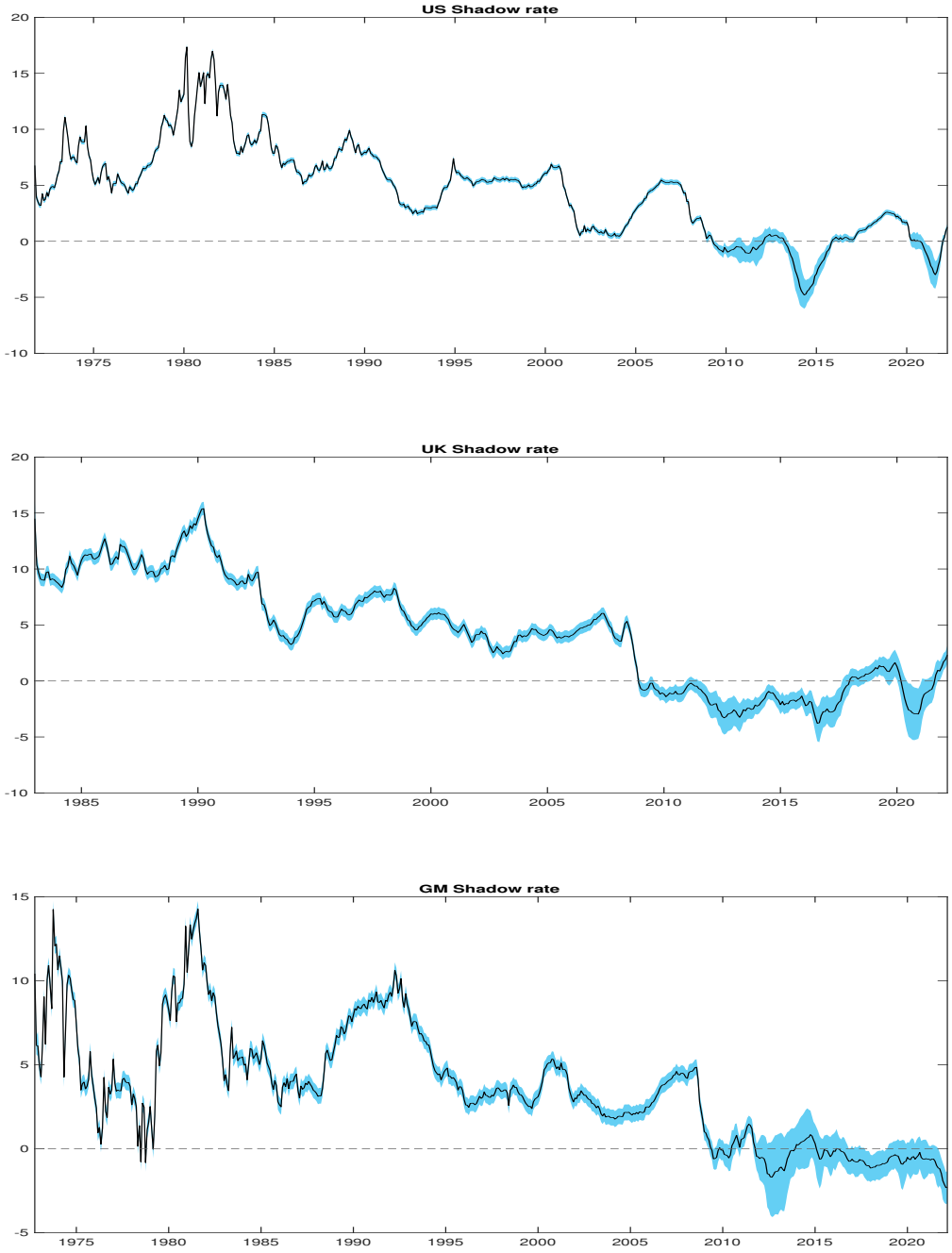

The solid lines are shadow rates and shaded areas are 90%-confidence intervals

Figure 2: **The real interest rate trend for US, UK and GM**

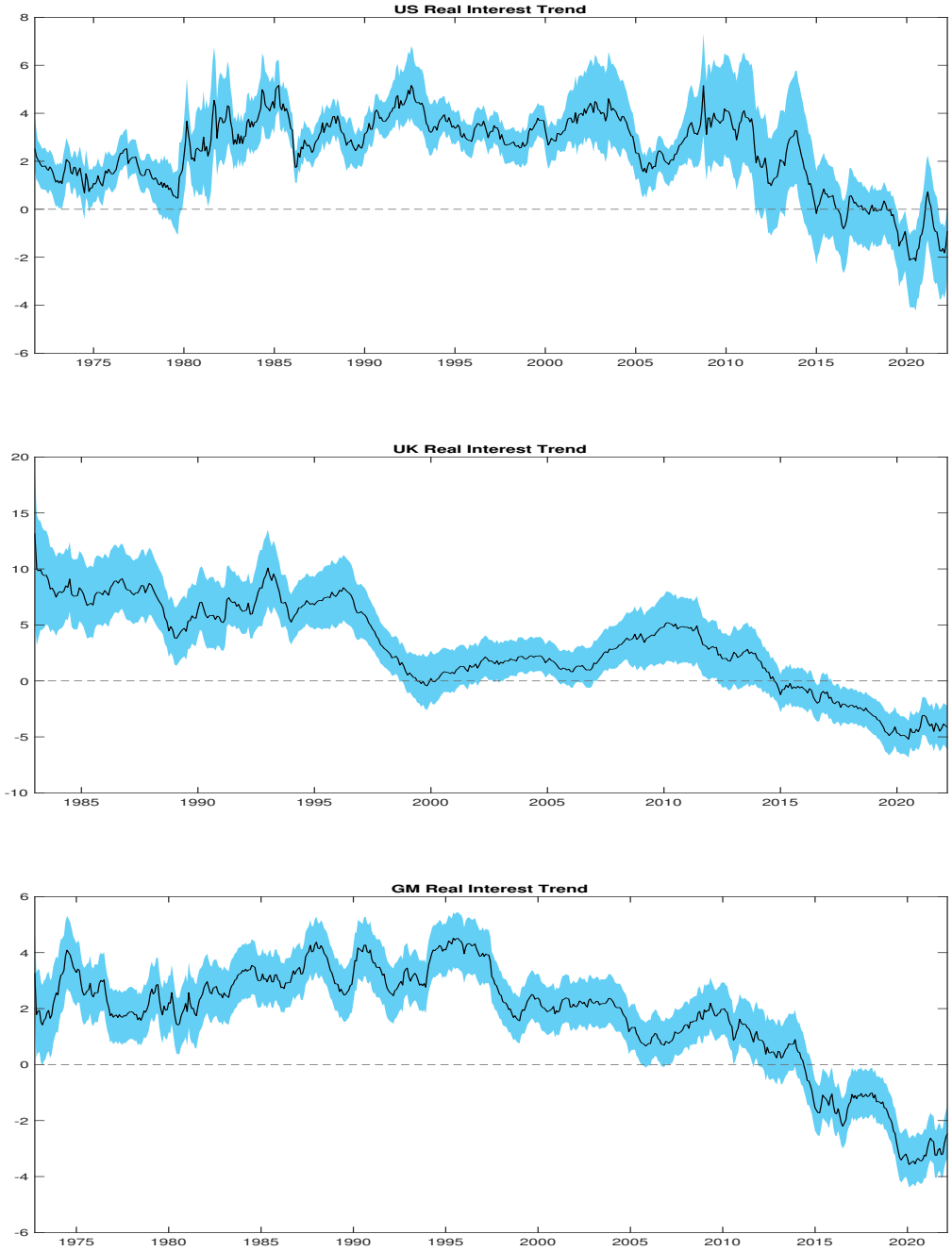

The solid lines are real interest rate trends and shaded areas are 90%-confidence intervals

Figure 3: **Variance decomposition of real interest rate trend with ordering of US,GM,UK**

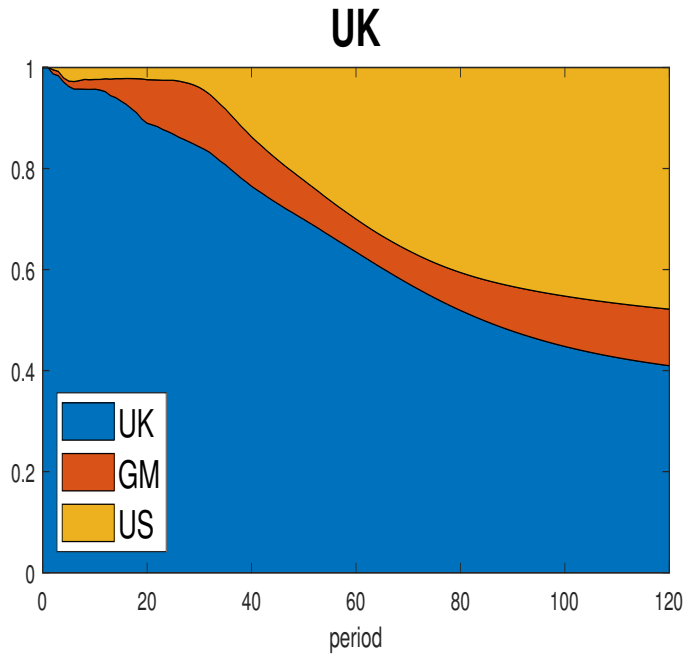

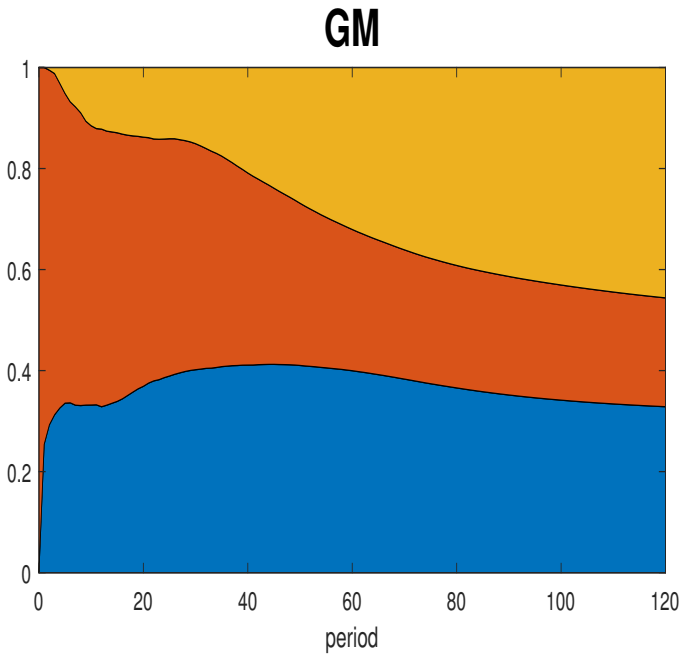

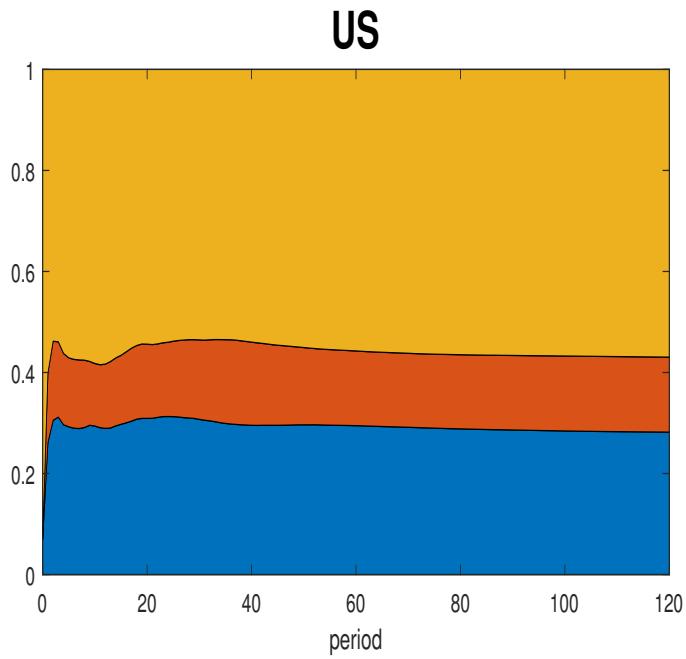

Figure 4: **Forecasts of shadow rate for US**

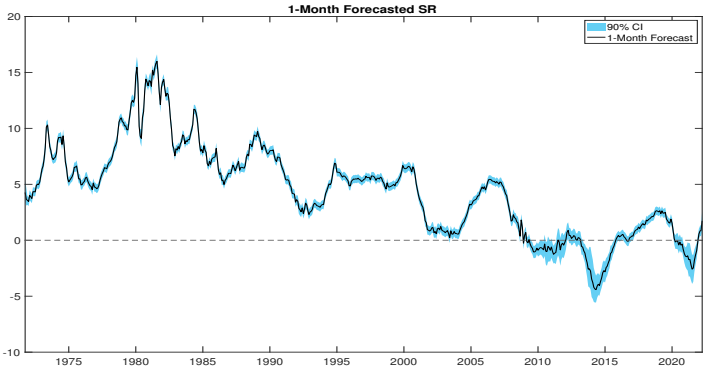

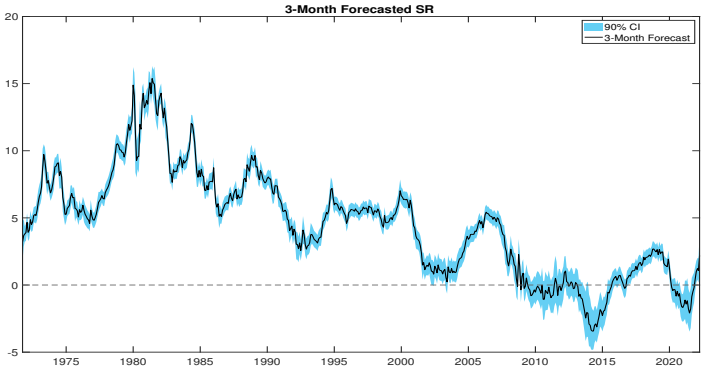

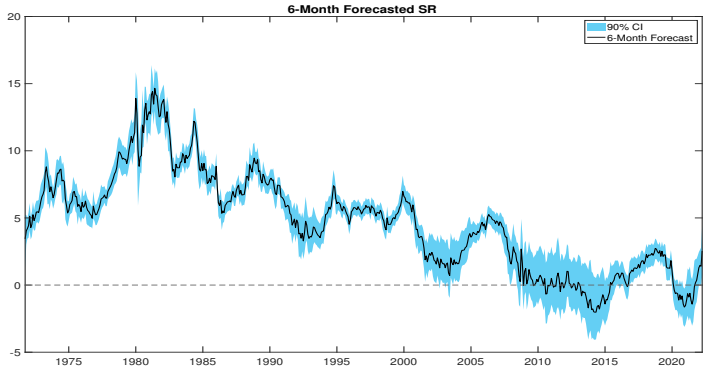

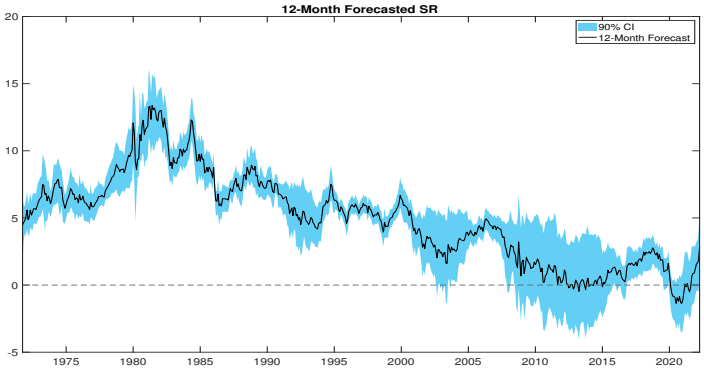

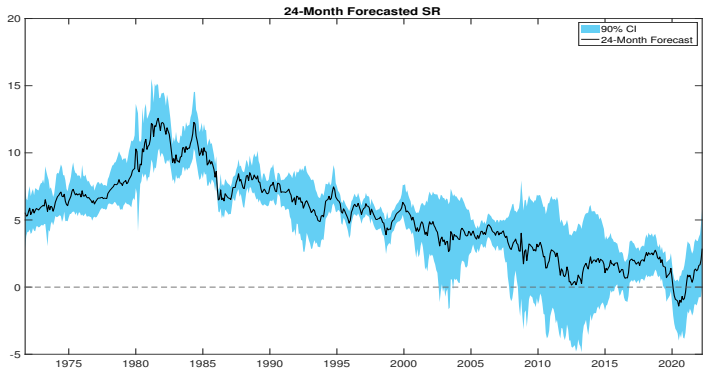

At each period t, we show forecasted shadow rate s_{t+h} using information up to t. Shaded areas are 90%-confidence intervals

Figure 5: **Forecast probability of zero lower bound for US**

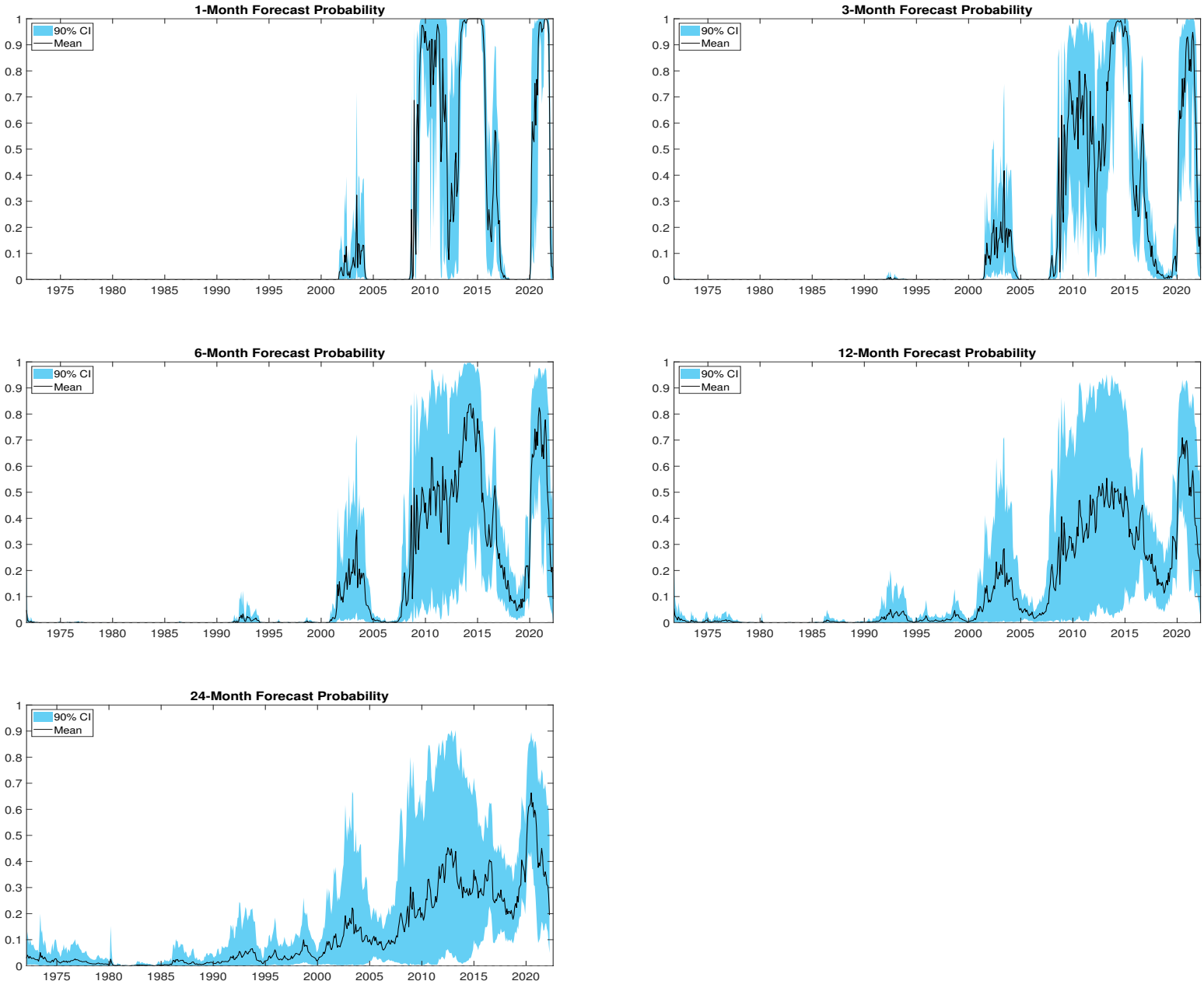

For the plot of h-Month Forecast Probability, at each period t we show the medium probability and confidence intervals that the ZLB will be binding at t+h. Shaded areas are 90%-confidence intervals

Figure 6: **Term premium on ten-year bonds**

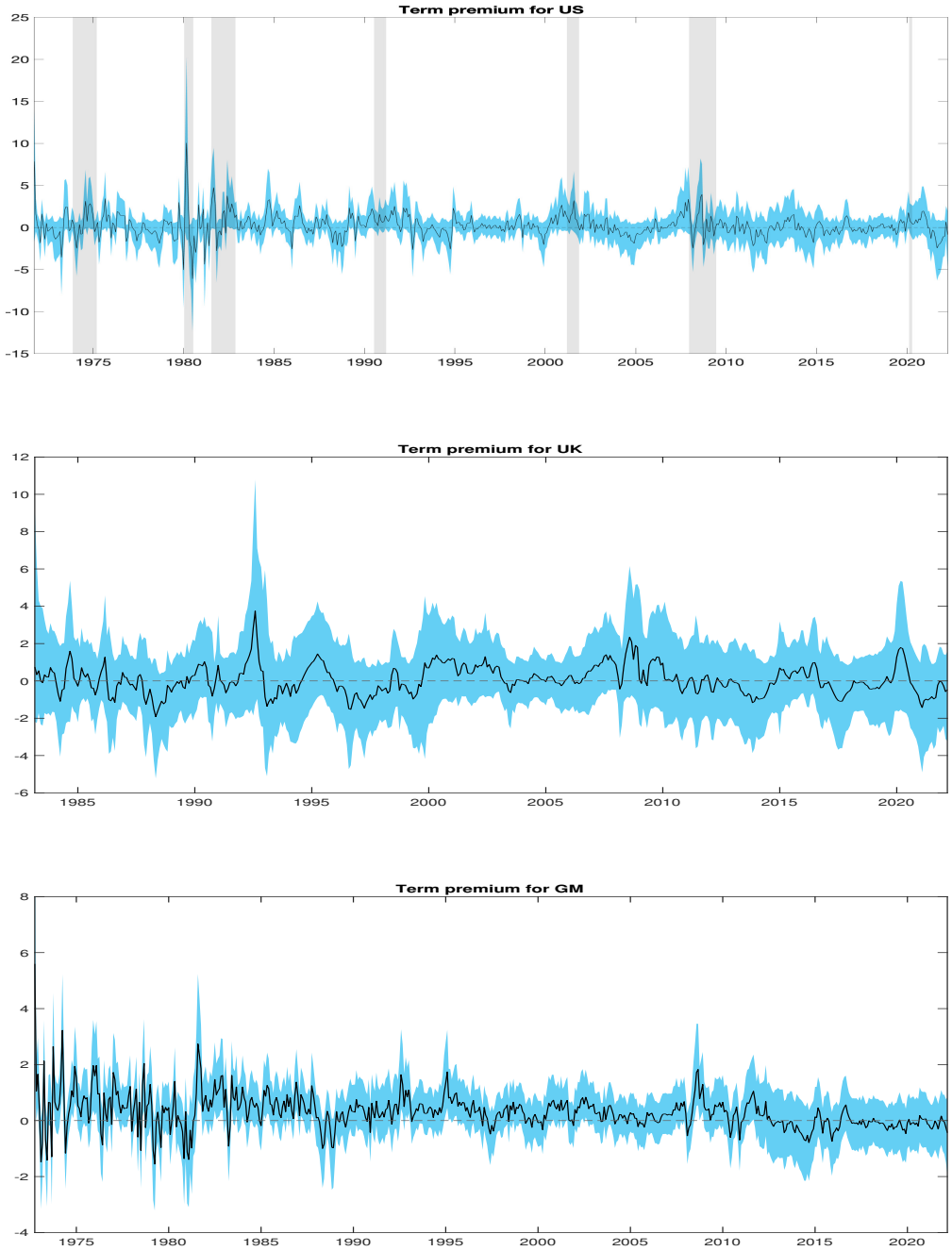

The solid lines are term premiums and blue shaded areas are 90%-confidence intervals. Gary shaded areas correspond to NBER recessions

Figure 7: **Coefficients of regressing excess return on forward rates**

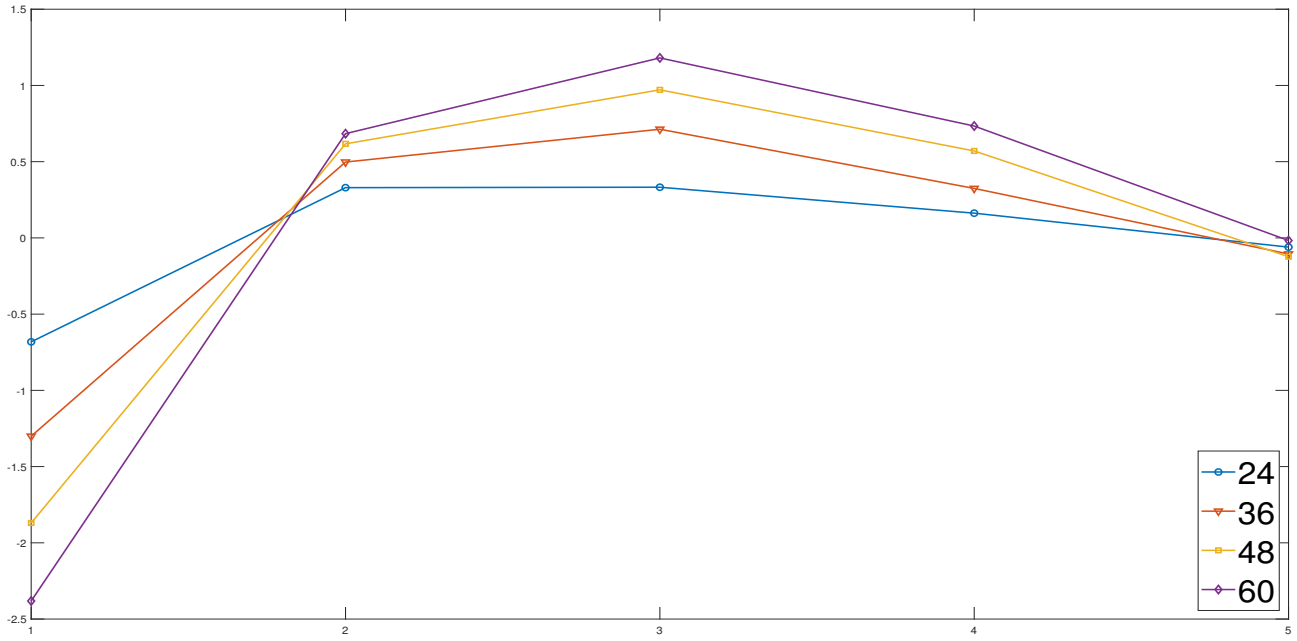

The regression equation is: $rx^m_{t+12} = b_0 + b_1\hat{y}^s_{t,12} + b_2\hat{f}^s_{t,12} + b_3\hat{f}^s_{t,24} + b_4\hat{f}^s_{t,36} + b_5\hat{f}^s_{t,48}$. The x axis represents the subscript of coefficients $[b_1, b_2, b_3, b_4, b_5]$. Each line corresponds to a regression regarding m-month yield excess return, where m = 24, 36,48, 60 as shown in the legend.

Appendix A Derivation of forward rates with lower bound

In GATSM equipped with a shadow rate, the bond prices are

$$P_t^m = exp(A_m + B_m' \cdot X_t) \tag{A.1}$$

$$s_t = \delta_0 + \delta_1' \cdot X_t \tag{A.2}$$

where

$$A_m = A_{m-1} + B_{m-1}'\mu^Q + \frac{1}{2}B_{m-1}'\Sigma\Sigma' B_{m-1} - \delta_0 \tag{A.3}$$

$$B_m' = -\delta_1' \sum_{j=0}^{m-1} (\Phi^Q)^j \tag{A.4}$$

The *shadow* forward rate in a world in which the lower bound is not binding is:

$$\begin{aligned} f_{t,m} &= p_t^m - p_t^{m+1} \\ &= (A_m - A_{m+1}) + (B_m - B_{m+1}) \cdot X_t \\ &= \delta_1' \sum_{j=0}^{m-1} (\Phi^Q)^j \mu^Q + \delta_0 - \frac{1}{2}\delta_1' \left(\sum_{j=0}^{m-1} (\Phi^Q)^j \right) \Sigma\Sigma' \left(\sum_{j=0}^{m-1} (\Phi^Q)^j \right)' \delta_1 + \delta_1' (\Phi^Q)^m X_t \\ &= \tilde{A}_m + \tilde{B}_m' \cdot X_t \end{aligned} \tag{A.5}$$

where p_t^m and p_t^{m+1} are the natural logs of the bond prices.

The conditional expectation of the future shadow rate under Q-measure is:

$$\begin{aligned} E_t^Q(s_{t+m}) &= \delta_0 + \delta_1' \cdot E_t^Q(X_{t+m}) \\ &= \delta_0 + \delta_1' \left\{ \sum_{j=0}^{m-1} (\Phi^Q)^j \mu^Q + (\Phi^Q)^m \cdot X_t \right\} \\ &= f_{t,m} + \frac{1}{2}\delta_1' \left(\sum_{j=0}^{m-1} (\Phi^Q)^j \right) \Sigma\Sigma' \left(\sum_{j=0}^{m-1} (\Phi^Q)^j \right)' \delta_1 \qquad \text{(A.6)} \\ &= f_{t,m} + CAT_m \qquad \text{(A.7)} \end{aligned}$$

where we define the second term in equation (A.6) as the convexity adjustment term (CAT_m). Therefore, the expectation of the future shadow rate under Q-measure can be expressed as a summation of the shadow forward rate and CAT_m which is a maturity-specific but time-invariant constant. To simplify the derivation, we define the adjusted shadow rate $\tilde{s}_{t+m} = s_{t+m} - CAT_m$, and equation (A.7) readily yields:

$$f_{t,m} = E_t^Q\left(\tilde{s}_{t+m}\right) \qquad \text{(A.8)}$$

Note that this is similar to equation (4.5) in Krippner (2015) under the forward measure in his continuous-time framework.

The conditional second moment of s_{t+m} (and $\tilde{s}_{t+m}$) under the Qmeasure, denoted by σ_m^2, is:

$$\begin{aligned} \sigma_m^2 = Var_t^Q(s_{t+m}) &= Var_t^Q\big(s_{t+m} - E_t^Q(s_{t+m})\big) \\ &= Var_t^Q\big(\delta_1'(u_{t+m}^Q + \Phi^Q u_{t+m-1}^Q + \cdots + (\Phi^Q)^{m-1} u_{t+1}^Q)\big) \\ &= \delta_1' \left(\sum_{j=0}^{m-1} (\Phi^Q)^j \Sigma\Sigma' (\Phi^{Q'})^j \right) \delta_1 \qquad \text{(A.9)} \end{aligned}$$

Consequently, under the risk-neutral measure, the adjusted future shadow rate $\tilde{s}_{t+m}$ follows a conditional normal distribution with mean $f_{t,m}$ and variance σ_m^2 as described above.

We denote the effective forward rate when the short rate is subject to the lower bound as $\underline{f}_{t,m}$. The no-arbitrage condition suggests approximately a risk-neutral pricing relationship between the effective forward rate and the actual short rate subject to the lower bound:

$$\underline{f}_{t,m} \approx E_t^Q(i_{t+m}) - \widetilde{CAT}_{t,m} \tag{A.10}$$

$$= E_t^Q(max(\underline{i}, s_{t+m})) - \widetilde{CAT}_{t,m} \tag{A.11}$$

where the first line involves the first-order approximation error, as demonstrated in equation (A.1) in Wu and Xia (2016). Note that a similar approximation to yield equation (4.8) in Krippner (2015) is not made explicit. This is because when the short rate is subject to a lower bound, its underlying distribution is not Gaussian, or it does not follow a well-defined Brownian motion in a continuous-time setting. Consequently, the usual change of measure operation cannot go through directly. Additionally, the term $\widetilde{CAT}_{t,m}$ reflects the convexity adjustment term for the actual short rate, which can be shown to become the time-invariant convexity adjustment term CAT_m in (A.7) if i_{t+m} is completely Gaussian or $i_{t+m} = s_{t+m}$.

Under those conditions the following approximation holds:

$$\underline{f}_{t,m} \approx E_t^Q(max(\underline{i}, \tilde{s}_{t+m})) \tag{A.12}$$

Then it is straightforward to derive the analytical form of the effective forward rate:

$$
\begin{aligned}
\underline{f}_{t,m} &\approx E_t^Q(max(\underline{i}, \tilde{s}_{t+m})) \\
&= E_t^Q[max(\underline{i},\ (s_{t+m} - CAT_m))] \\
&= E_t^Q(s_{t+m} - CAT_m) + E_t^Q[max(\underline{i} - (s_{t+m} - CAT_m),\ 0)] \\
&= f_{t,m} + \int_{-\infty}^{\infty} max(\underline{i} - s_{t+m} + CAT_m, 0) f(s_{t+m}) ds_{t+m} \\
&= f_{t,m} + \int_{-\infty}^{\underline{i}+CAT_m} (\underline{i} - s_{t+m} + CAT_m) \frac{1}{\sqrt{2\pi\sigma_m^2}} exp\bigg[-\frac{1}{2}\bigg(\frac{s_{t+m} - E_t^Q(s_{t+m})}{\sigma_m}\bigg)^2\bigg] ds_{t+m} \\
&= f_{t,m} + z_{t,m}
\end{aligned}
\tag{A.13}
$$

We define $\mu = E_t^Q(s_{t+m}) = f_{t,m} + CAT_m$ and $y = s_{t+m}$; then, the analytical form of $z_{t,m}$ can be further derived as:

$$
\begin{aligned}
z_{t,m} &= \int_{-\infty}^{\underline{i}+CAT_m} (\underline{i} + CAT_m - y) \frac{1}{\sqrt{2\pi\sigma_m^2}} exp\bigg[-\frac{1}{2}\bigg(\frac{y-\mu}{\sigma_m}\bigg)^2\bigg] dy \\
&= \int_{-\infty}^{\underline{i}+CAT_m} (\underline{i} + CAT_m - y) \frac{1}{\sqrt{2\pi}} exp\bigg[-\frac{1}{2}\bigg(\frac{y-\mu}{\sigma_m}\bigg)^2\bigg] d\bigg(\frac{y-\mu}{\sigma_m}\bigg) \\
&= \int_{-\infty}^{\frac{\underline{i}+CAT_m-\mu}{\sigma_m}} (\underline{i} + CAT_m - \mu - \sigma_m x) \frac{1}{\sqrt{2\pi}} exp\bigg(-\frac{1}{2}x^2\bigg) dx \\
&= (\underline{i} + CAT_m - \mu) \int_{-\infty}^{\frac{\underline{i}+CAT_m-\mu}{\sigma_m}} \frac{1}{\sqrt{2\pi}} exp\bigg(-\frac{1}{2}x^2\bigg) dx \\
&- \sigma_m \int_{-\infty}^{\frac{\underline{i}+CAT_m-\mu}{\sigma_m}} x \frac{1}{\sqrt{2\pi}} exp\bigg(-\frac{1}{2}x^2\bigg) dx \\
&= (\underline{i} + CAT_m - \mu) \mathbf{\Phi}\bigg(\frac{\underline{i} + CAT_m - \mu}{\sigma_m}\bigg) + \sigma_m \frac{1}{\sqrt{2\pi}} \int_{-\infty}^{\frac{\underline{i}+CAT_m-\mu}{\sigma_m}} exp\bigg(-\frac{1}{2}x^2\bigg) d\bigg(\frac{-x^2}{2}\bigg) \\
&= (\underline{i} + CAT_m - \mu) \mathbf{\Phi}\bigg(\frac{\underline{i} + CAT_m - \mu}{\sigma_m}\bigg) + \sigma_m \frac{1}{\sqrt{2\pi}} exp\bigg[-\frac{1}{2}\bigg(\frac{\underline{i} + CAT_m - \mu}{\sigma_m}\bigg)^2\bigg] \\
&= (\underline{i} - f_{t,m}) \bigg[1 - \mathbf{\Phi}\bigg(\frac{f_{t,m} - \underline{i}}{\sigma_m}\bigg)\bigg] + \sigma_m \phi\bigg(\frac{f_{t,m} - \underline{i}}{\sigma_m}\bigg)
\end{aligned}
\tag{A.14}
$$

where the third equality follows by defining $x = \frac{y-\mu}{\sigma_m}$ and the last equality is obtained using (A.7). Finally, $\mathbf{\Phi}(\cdot)$ and $\phi(\cdot)$ are the cumulative distribution function and the probability density function of the standard normal distribution, respectively. Substituting equation (A.14) into equation (A.13), we obtain the final analytical form of $\underline{f}_{t,m}$:

$$\begin{aligned}
\underline{f}_{t,m} &= f_{t,m} + (\underline{i} - f_{t,m})\left[1 - \mathbf{\Phi}\left(\frac{f_{t,m} - \underline{i}}{\sigma_m}\right)\right] + \sigma_m \boldsymbol{\phi}\left(\frac{f_{t,m} - \underline{i}}{\sigma_m}\right) \\
&= \underline{i} + (f_{t,m} - \underline{i})\mathbf{\Phi}\left(\frac{f_{t,m} - \underline{i}}{\sigma_m}\right) + \sigma_m \boldsymbol{\phi}\left(\frac{f_{t,m} - \underline{i}}{\sigma_m}\right) \\
&= \underline{i} + \sigma_m \left[\frac{(f_{t,m} - \underline{i})}{\sigma_m} \cdot \mathbf{\Phi}\left(\frac{f_{t,m} - \underline{i}}{\sigma_m}\right) + \boldsymbol{\phi}\left(\frac{f_{t,m} - \underline{i}}{\sigma_m}\right)\right] \\
&= \underline{i} + \sigma_m g\left(\frac{f_{t,m} - \underline{i}}{\sigma_m}\right)
\end{aligned} \tag{A.15}$$

We note that the conditions under which the above derivations can go through can be concisely summarized as the following requirement of the term $\widetilde{CAT}_{t,m}$:

$$\widetilde{CAT}_{t,m} = \sigma_m g\left[\frac{(f_{t,m} - (\underline{i} - CAT_m))}{\sigma_m}\right] - \sigma_m g\left[\frac{f_{t,m} - \underline{i}}{\sigma_m}\right] \tag{A.16}$$

To illustrate this, the work on equation (A.11) is as follows:

$$\begin{aligned}
\underline{f}_{t,m} &= E_t^Q(max(\underline{i}, s_{t+m})) - \widetilde{CAT}_{t,m} \\
&= E_t^Q(s_{t+m}) + E_t^Q(max(\underline{i} - s_{t+m}, 0)) - \widetilde{CAT}_{t,m} \\
&= E_t^Q(s_{t+m}) + E_t^Q(max(\underline{i} - CAT_m - (s_{t+m} - CAT_m), 0)) - \widetilde{CAT}_{t,m} \\
&= E_t^Q(s_{t+m}) + (\underline{i}^* - f_{t,m})\left[1 - \mathbf{\Phi}\left(\frac{f_{t,m} - \underline{i}^*}{\sigma_m}\right)\right] + \sigma_m \phi\left(\frac{f_{t,m} - \underline{i}^*}{\sigma_m}\right) - \widetilde{CAT}_{t,m} \\
&= \underline{i} - \widetilde{CAT}_{t,m} + \sigma_m g\left(\frac{f_{t,m} - (\underline{i} - CAT_m)}{\sigma_m}\right)
\end{aligned} \tag{A.17}$$

where the fourth equality uses the integral result in (A.14), with $\underline{i}^* = \underline{i} - CAT_m$ replacing $\underline{i}$, and the last equality uses $E_t^Q(s_{t+m}) = f_{t,m} + CAT_m$. Taking the difference between (A.17)

and (A.15), we obtain (A.16).

Note that in (A.16), when the short rate is far above the lower bound, we have $\mathbf{\Phi}(\cdot) \to 1$ and $\phi(\cdot) \to 0$ in the limit; that is, when $\widetilde{CAT}_{t,m}$ becomes exactly CAT_m and (A.10) coincides with (A.7).

Although our derivation is similar to Krippner (2015) in that we also work directly on the mapping between the forward rates and expected future short rates, we operate under the risk-neutral measure instead of relying on the forward measure in a continuous-time framework, as in his derivation. We also corroborate Wu and Xia (2016) in highlighting the necessary approximations owing to the non-Gaussian feature of the effective forward rate and short rate when the lower bound is binding.

Finally, we note that this analytical form is robust to the DTSM with drifting trends as long as the conditional distribution of $\tilde{s}_{t+m}$ is well defined. Therefore, the same analytical form appears to be valid theoretically even when the unit roots are present in the risk-neutral process as well as the physical process so long as the consol bond is excluded from consideration.

Appendix B Prior Distributions

Table B1: Prior distribution for parameters in three countries

Panel A

US	Distribution	Values
σ_τ^2	$IG(\alpha_\eta/2,\ \delta_\eta/2)$	$\alpha_\eta = 100,\ \delta_\eta = 0.16(\alpha_\eta - 2)$
$\Sigma\Sigma'$	$IW(\kappa,\ \Psi)$	$\kappa = 5,\ \Psi = (\kappa - 4)\tilde{\Omega}$
		$\tilde{\Omega}$ from classical estimation
Φ	$N(\bar{\Phi},\ \Omega_\Phi)$	Minnesota prior
γ	$N(\mu_\gamma,\ \Omega_\gamma)$	$\mu_\gamma = [-0.42,\ -0.12]'$
		$\Omega_\gamma = diag(0.01, 0.01)$
$\bar{X}$	$N(\mu_X,\ \Omega_X)$	$\mu_X = [2.83,\ 1.00]'$
		$\Omega_X = diag(1, 1)$
σ_e^2	$IG(\alpha_e/2,\ \delta_e/2)$	$\alpha_e = 4, \quad \delta_e = 0.01(\alpha_e - 2)$
k_∞^Q	$N(\mu_k,\ \sigma_k^2)$	$\mu_k = 0.03, \quad \sigma_k^2 = 0.02^2$
$\sigma_{\eta\pi}^2$	$IG(\alpha_{\eta\pi}/2,\ \delta_{\eta\pi}/2)$	$\alpha_{\eta\pi} = 4,\ \delta_{\eta\pi} = 0.01(\alpha_{\eta\pi} - 2)$
$\sigma_{\pi c}^2$	$IG(\alpha_{\pi c}/2,\ \delta_{\pi c}/2)$	$\alpha_{\pi c} = 4,\ \delta_{\pi c} = 0.02(\alpha_{\pi c} - 2)$
$\sigma_{\pi s}^2$	$IG(\alpha_{\pi s}/2,\ \delta_{\pi s}/2)$	$\alpha_{\pi s} = 4,\ \delta_{\pi s} = 0.002(\alpha_{\pi s} - 2)$
ϕ_1	$N(\mu_1,\ \sigma_{\mu 1}^2)$	$\phi_1 = 1.40,\ \sigma_{\mu 1}^2 = 4$
ϕ_2	$N(\mu_2,\ \sigma_{\mu 2}^2)$	$\phi_2 = -0.45,\ \sigma_{\mu 2}^2 = 4$

IG means a inverse Gamma distribution. *IW* is inverse-Wishart distribution. *N* refers to Normal distribution. Priors for parameters not listed in the table are completely uninformative. $\sigma_\tau^2 = \sigma_{\eta r}^2 + \sigma_{\eta\pi}^2$ according to Equation (6). And we use σ_τ^2 to pin down $\sigma_{\eta r}^2$ in our estimation.

Panel B

UK	Distribution	Values
σ_τ^2	$IG(\alpha_\eta/2,\ \delta_\eta/2)$	$\alpha_\eta = 100,\ \delta_\eta = 0.10(\alpha_\eta - 2)$
$\Sigma\Sigma'$	$IW(\kappa,\ \Psi)$	$\kappa = 5, \Psi = (\kappa - 4)\tilde{\Omega}$
		$\tilde{\Omega}$ from classical estimation
Φ	$N(\bar{\Phi},\ \Omega_\Phi)$	Minnesota prior
γ	$N(\mu_\gamma,\ \Omega_\gamma)$	$\mu_\gamma = [-1.50,\ 0.06]'$
		$\Omega_\gamma = diag(0.01, 0.01)$
$\bar{X}$	$N(\mu_X,\ \Omega_X)$	$\mu_X = [3.79,\ -0.14]'$
		$\Omega_X = diag(1, 1)$
σ_e^2	$IG(\alpha_e/2,\ \delta_e/2)$	$\alpha_e = 4, \quad \delta_e = 0.01(\alpha_e - 2)$
k_∞^Q	$N(\mu_k,\ \sigma_k^2)$	$\mu_k = 0.04, \quad \sigma_k^2 = 0.02^2$
$\sigma_{\eta\pi}^2$	$IG(\alpha_{\eta\pi}/2,\ \delta_{\eta\pi}/2)$	$\alpha_{\eta\pi} = 4,\ \delta_{\eta\pi} = (\alpha_{\eta\pi} - 2)$
$\sigma_{\pi c}^2$	$IG(\alpha_{\pi c}/2,\ \delta_{\pi c}/2)$	$\alpha_{\pi c} = 4,\ \delta_{\pi c} = 0.01(\alpha_{\pi c} - 2)$
$\sigma_{\pi s}^2$	$IG(\alpha_{\pi s}/2,\ \delta_{\pi s}/2)$	$\alpha_{\pi s} = 4,\ \delta_{\pi s} = 100(\alpha_{\pi c} - 2)$
ϕ_1	$N(\mu_1,\ \sigma_{\mu 1}^2)$	$\phi_1 = 1.20,\ \sigma_{\mu 1}^2 = 4$
ϕ_2	$N(\mu_2,\ \sigma_{\mu 2}^2)$	$\phi_2 = -0.50,\ \sigma_{\mu 2}^2 = 4$

Panel C

Germany	Distribution	Values
σ_τ^2	$IG(\alpha_\eta/2,\ \delta_\eta/2)$	$\alpha_\eta = 100,\ \delta_\eta = 0.02(\alpha_\eta - 2)$
$\Sigma\Sigma'$	$IW(\kappa,\ \Psi)$	$\kappa = 5, \Psi = (\kappa - 4)\tilde{\Omega}$
		$\tilde{\Omega}$ from classical estimation
Φ	$N(\bar{\Phi},\ \Omega_\Phi)$	Minnesota prior
γ	$N(\mu_\gamma,\ \Omega_\gamma)$	$\mu_\gamma = [-1.50,\ 0.18]'$
		$\Omega_\gamma = diag(0.01, 0.01)$
$\bar{X}$	$N(\mu_X,\ \Omega_X)$	$\mu_X = [-1.17,\ 0.90]'$
		$\Omega_X = diag(1, 1)$
σ_e^2	$IG(\alpha_e/2,\ \delta_e/2)$	$\alpha_e = 4, \quad \delta_e = 0.04(\alpha_e - 2)$
k_∞^Q	$N(\mu_k,\ \sigma_k^2)$	$\mu_k = 0.02, \quad \sigma_k^2 = 0.02^2$
$\sigma_{\eta\pi}^2$	$IG(\alpha_{\eta\pi}/2,\ \delta_{\eta\pi}/2)$	$\alpha_{\eta\pi} = 4,\ \delta_{\eta\pi} = (\alpha_{\eta\pi} - 2)$
$\sigma_{\pi c}^2$	$IG(\alpha_{\pi c}/2,\ \delta_{\pi c}/2)$	$\alpha_{\pi c} = 4,\ \delta_{\pi c} = 0.01(\alpha_{\pi c} - 2)$
$\sigma_{\pi s}^2$	$IG(\alpha_{\pi s}/2,\ \delta_{\pi s}/2)$	$\alpha_{\pi s} = 4,\ \delta_{\pi s} = 100(\alpha_{\pi s} - 2)$
ϕ_1	$N(\mu_1,\ \sigma_{\mu 1}^2)$	$\phi_1 = 0.6,\ \sigma_{\mu 1}^2 = 4$
ϕ_2	$N(\mu_2,\ \sigma_{\mu 2}^2)$	$\phi_2 = 0.2,\ \sigma_{\mu 2}^2 = 4$

Appendix C Derivation of Term Premium

The term premium of yield with m-period maturity at time t, TP_t^m, is defined as

$$TP_{t+1}^m = my_{t,m} - (m-1)y_{t+1,m-1} - y_{t,1} \tag{C.1}$$

where $y_{t,1}$ denotes the short rate at time t. In our unspanned DTSM, the yield is affine in latent factors and maintains no-arbitrage constraints. Thus, we have[18]

$$\begin{aligned}
y_{t,m} &= -\frac{1}{m}\bar{A}_m - \frac{1}{m}(\bar{B}_m', 0, 0)\cdot(X_t',\ r_t^*,\ \pi_t^*)' \\
\bar{B}_m' &= \bar{B}_{m-1}'\Phi^Q - \delta_1' \\
\bar{A}_m &= \bar{A}_{m-1} + \bar{B}_{m-1}'\mu^Q + \frac{1}{2}(\bar{B}_{m-1}', 0, 0)\Omega(\bar{B}_{m-1}', 0, 0)' - \delta_0 \\
\Omega &= \begin{pmatrix} \Sigma\Sigma' & \gamma\sigma_{\eta r}^2 & \gamma\sigma_{\eta\pi}^2 \\ \gamma'\sigma_{\eta r}^2 & \sigma_{\eta r}^2 & 0 \\ \gamma'\sigma_{\eta\pi}^2 & 0 & \sigma_{\eta\pi}^2 \end{pmatrix}
\end{aligned} \tag{C.2}$$

Substituting (C.2) into (C.1), plugging in the physical process of factors in equation (7), and the risk price in equation (10), and taking the expectation, we obtain the expected term premium on m-period yield[19]:

$$\begin{aligned}
E_t(TP_{t+1}^m) &= \bar{B}_{m-1}'[(I_3-\Phi)\bar{X} - \mu^Q + (\Phi-\Phi^Q,\ (I_3-\Phi)\gamma,\ (I_3-\Phi)\gamma)\cdot(X_t',\ r_t^*,\ \pi_t^*)'] \\
&\quad - \frac{1}{2}(\bar{B}_{m-1}', 0, 0)\Omega(\bar{B}_{m-1}', 0, 0)' \\
&= \bar{B}_{m-1}'[\lambda_0 + \lambda_1\cdot(X_t',\ r_t^*,\ \pi_t^*)'] - \frac{1}{2}(\bar{B}_{m-1}', 0, 0)\Omega(\bar{B}_{m-1}', 0, 0)'
\end{aligned} \tag{C.3}$$

[18] See Duffie and Kan (1996) for detailed proofs.

[19] In our analysis of the term premium we ignore the convexity adjustment term but focus on the first term of equation (C.3).

Appendix D Different Measures of Inflation Uncertainty

In this section, we estimate equation (39) using the other three measures of inflation uncertainty: the standard deviation of transitory shock from the UCSV model, the combination of the standard deviation of transitory shock and the standard deviation of permanent shock from the UCSV model, and the survey dispersion of inflation forecasts employed in Wright (2011). Specifically, the survey dispersion measure is the standard deviation of individual forecasts based on the Consensus Forecasts report of inflation forecasts that we do not have access to. Thus, we use the survey dispersion provided by Wright (2011) covering October 1989 to January 2009. All estimations in this sector are based on monthly data and the estimates of coefficient b are presented in Table A5. In the first column of Table A5, the s.d. of transitory shocks, as a single regressor, is negatively correlated with the term premium. The second column contains two explanatory variables in the regression. The coefficient of s.d. of permanent shock is positive and statistically significant, while the coefficient of s.d. of transitory shock is negative and significant. In the third column, we regress our estimates of the term premium on the same survey dispersion of inflation from Wright (2011) and obtain a negative, but insignificant coefficient.

Table A1: **Cointegrating vectors among latent factors**

Panel A: U.S.					
Γ	1	0	0	1.55 (0.20)	1.55 (0.20)
	0	1	0	−0.65 (0.17)	−0.65 (0.17)
	0	0	1	0.10 (0.15)	0.10 (0.15)
Panel B: U.K.					
Γ	1	0	0	2.27 (0.16)	2.27 (0.16)
	0	1	0	−1.60 (0.12)	−1.60 (0.12)
	0	0	1	0.32 (0.12)	0.32 (0.12)
Panel C: Germany					
Γ	1	0	0	1.96 (0.13)	1.96 (0.13)
	0	1	0	−1.35 (0.12)	−1.35 (0.12)
	0	0	1	0.39 (0.13)	0.39 (0.13)

There are five latent factors in our SDTSM, $(X_{1t}, X_{2t}, X_{3t}, r_t^*, \pi_t^*)$, and three cointegrating vectors. The 3×5 matrix, $\Gamma = [I_3, \gamma, \gamma]$, stacks cointegrating vectors in rows. According to the normalization in Section **??**, only the second and third elements in γ are freely estimated.

Table A2: **Cointegration: estimates of real interest rate trend**

Panel A			
	U.S.	U.K.	Germany
ADF test (p-value)	0.25	0.83	0.93
Panel B			
Johansen cointegration test	stat	p-value	h
r=0	63.40	0.00	1
r=1	32.34	0.01	1
r=2	5.48	0.58	0
Panel C			
VECM model with 2 cointegrating vectors			
Error-correction coefficients	0.78	−3.15	0.62
(S.E.)	(0.01)	(0.01)	(0.01)
	0.16	2.18	−1.74
	(0.01)	(0.01)	(0.01)

Note: The the number of lags in the ADF test is selected according to the AIC.

Table A3: **Correlation: term premium estimates**

Panel A

	1st PC	2nd PC	3rd PC
Principal Component Analysis			
Total variance explained (%)	66.45	26.25	7.30

Panel B

	US	UK	GM
Regress term premium on the first PC			
adjusted-R^2	0.91	0.36	0.22

Note: We use the overlapping sample period from Jan 1983 to Mar 2022 to analyze the correlation among term premium estimates across countries.

Table A4: **Forecast of economic recessions**

Panel A: In-sample	1-month		3-month		6-month		12-month	
	TP	ES	TP	ES	TP	ES	TP	ES
Coefficient	0.24	-0.09	0.25	-0.17	0.14	-0.27	0.04	-0.44
P-value	0.00	0.01	0.00	0.00	0.00	0.00	0.46	0.00
R-square	0.06	0.02	0.06	0.06	0.02	0.13	0.00	0.26
Correct Months	1	0	1	0	0	4	0	13
Panel B: Out-of-sample	1-month		3-month		6-month		12-month	
	TP	ES	TP	ES	TP	ES	TP	ES
RMSE	0.29	0.29	0.28	0.29	0.27	0.29	0.27	0.27
0|0	436	437	437	437	436	437	435	432
1|1	3	0	5	0	4	0	2	5

This table provides the results of economic recession in-sample and out-of-sample forecasting exercise for the U.S. data. TP is the term premium of ten-year yield derived from our model. ES represents the empirical slope, ten-year yield minus three-month yield.

Table A5: **Term premium and various measures of inflation uncertainty**

Regression of term premium on inflation uncertainty			
Regressors		Estimate	
S.D. of transitory shock	-0.79 (0.00)	-0.84 (0.00)	
S.D. of permanent shock		1.75 (0.01)	
Survey dispersion			-0.57 (0.05)

This table shows the estimates of b in equation (39) using different measures of inflation uncertainty as explanatory variables. The p-values in parenthesis are obtained from a block bootstrap. The regression involving survey dispersion covers the time period from October 1989 to January 2009. Other regressions use monthly data spanning from January 1983 to March 2022.

Figure A1: **Comparing shadow rates**

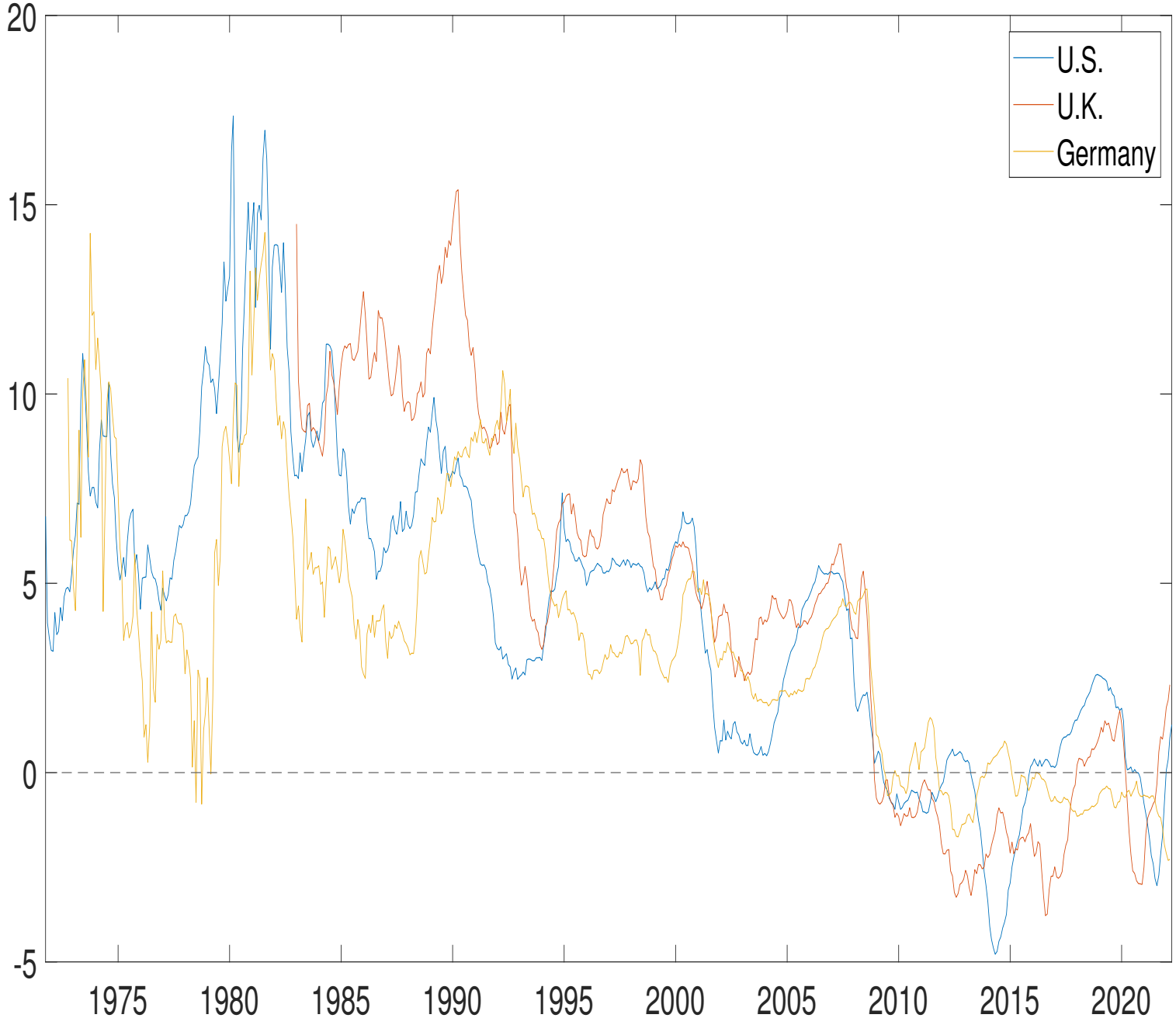

Figure A2: **Comparing real interest rate trends**

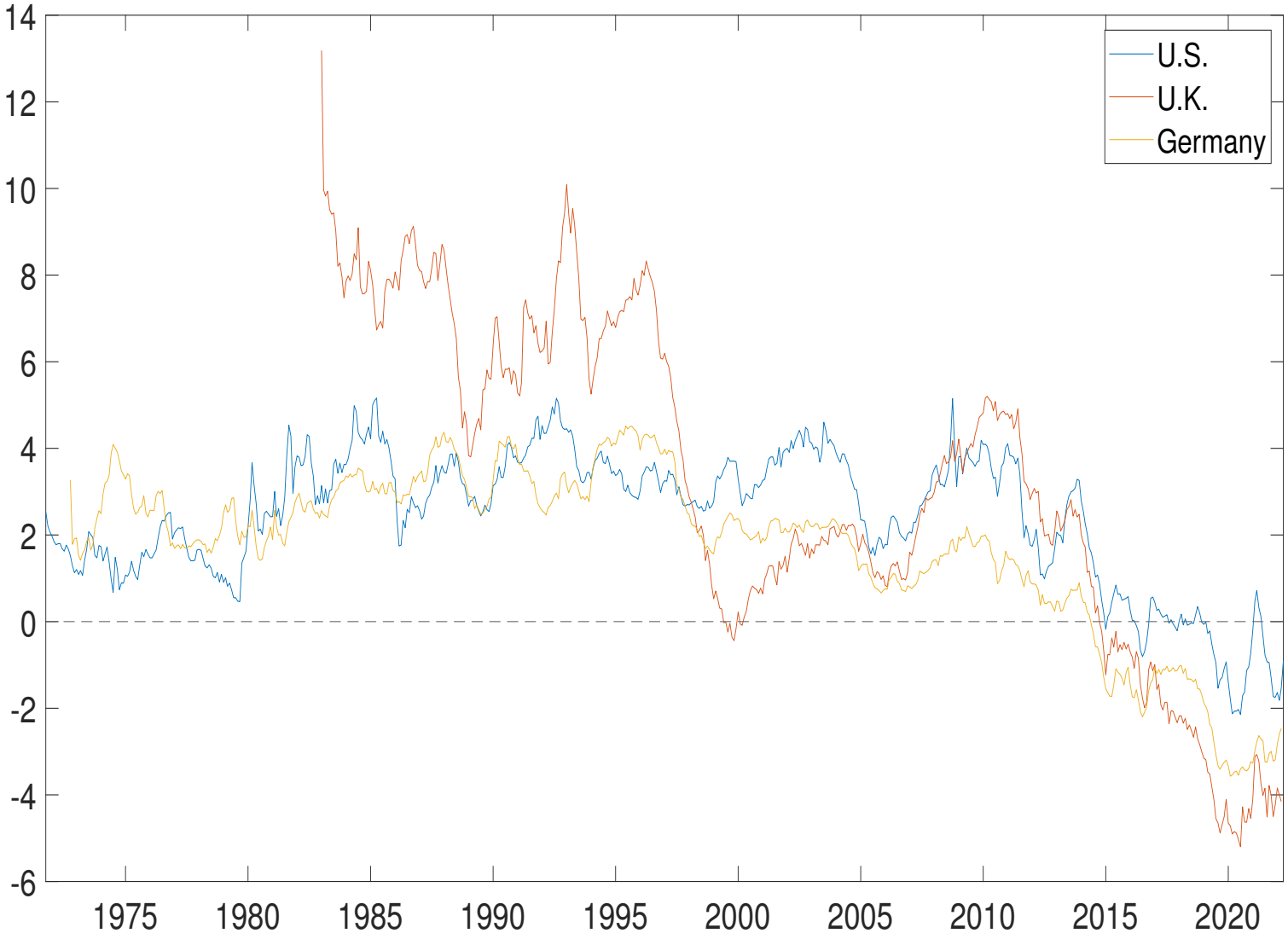

Figure A3: **The trend of shadow rate for US, UK, and GM**

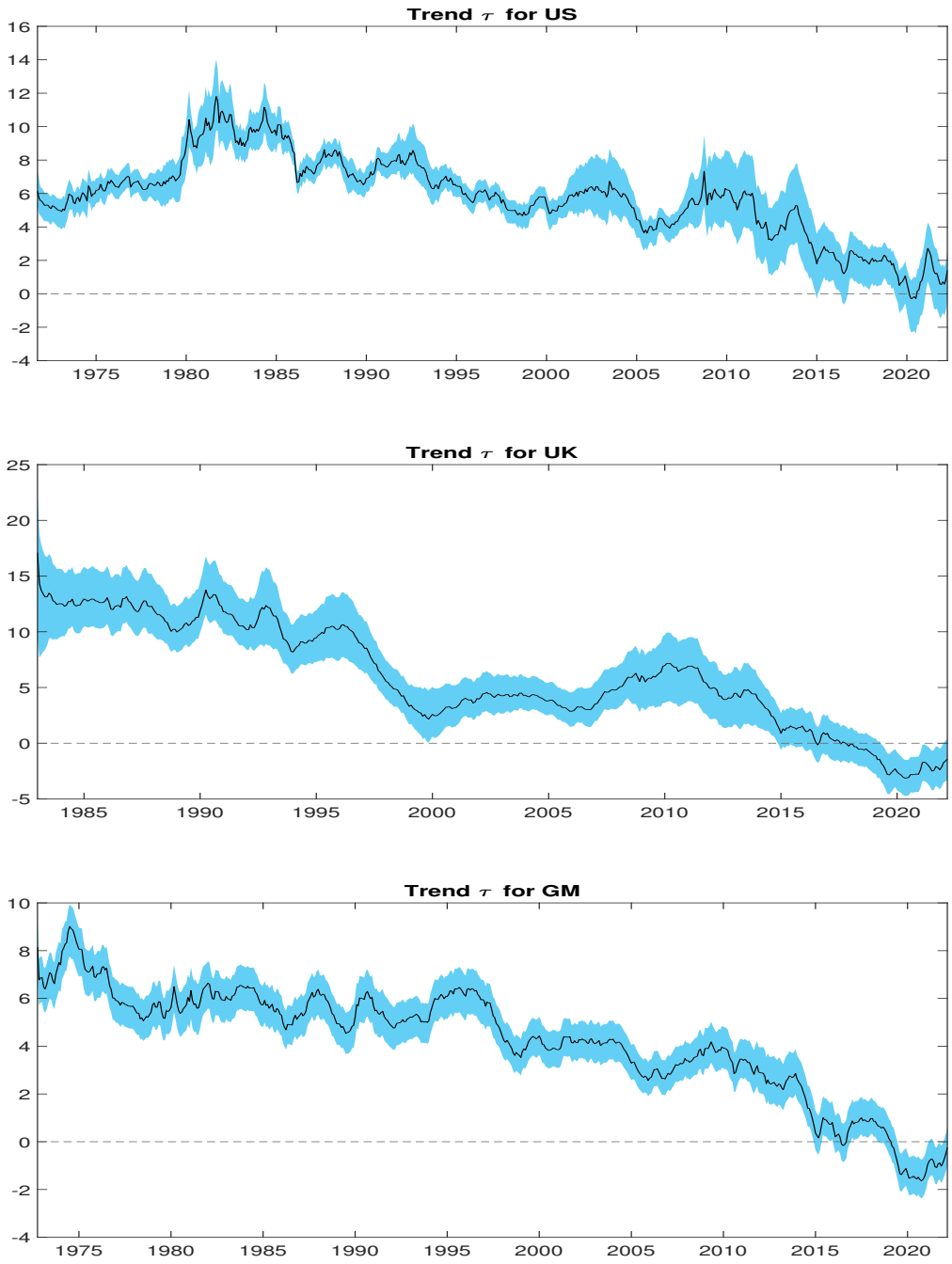

The solid lines are trends of shadow rate and shaded areas are 90%-confidence intervals

Figure A4: **Variance decomposition of real interest rate trends with ordering of GM, UK, US**

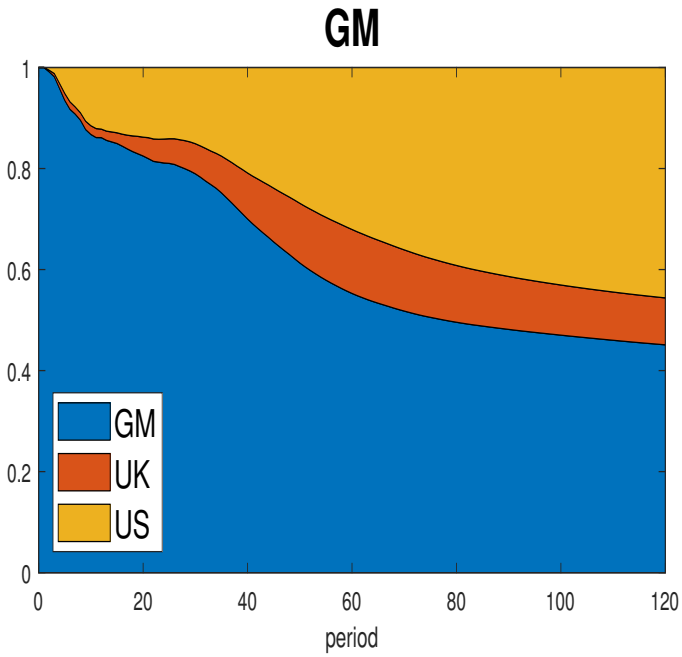

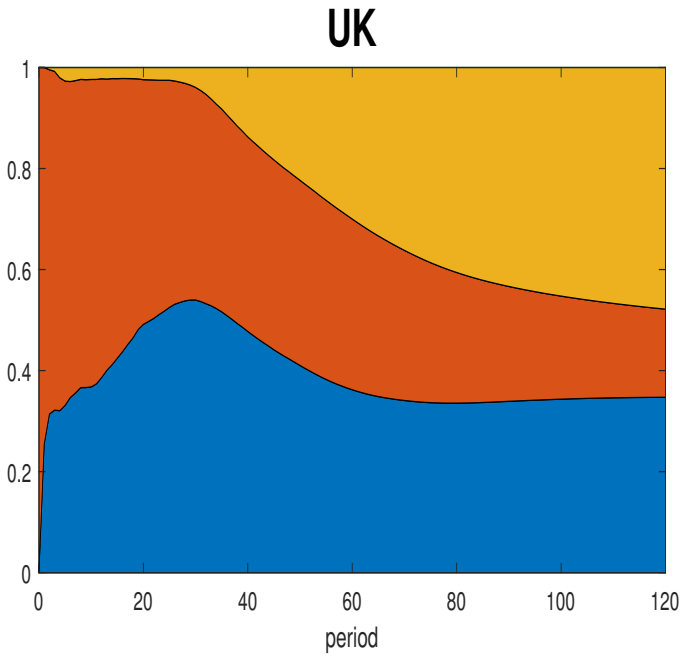

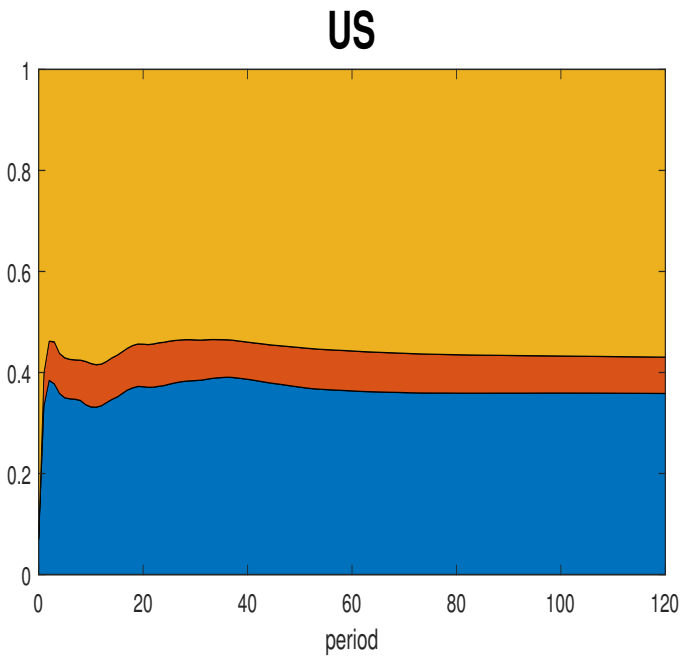

Figure A5: **Comparing term premiums**

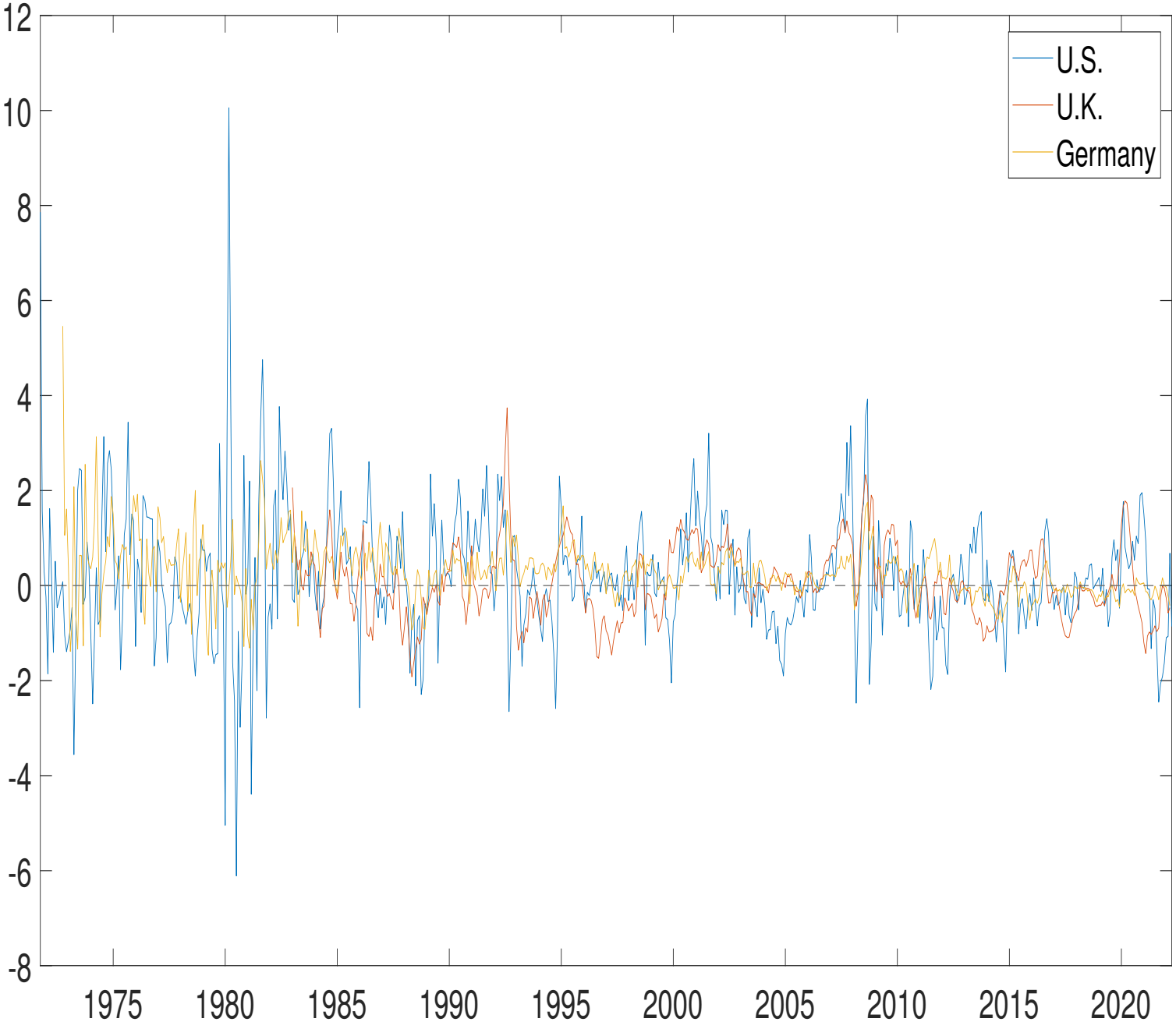

Figure A6: **Standard deviation of the permanent shock to inflation**

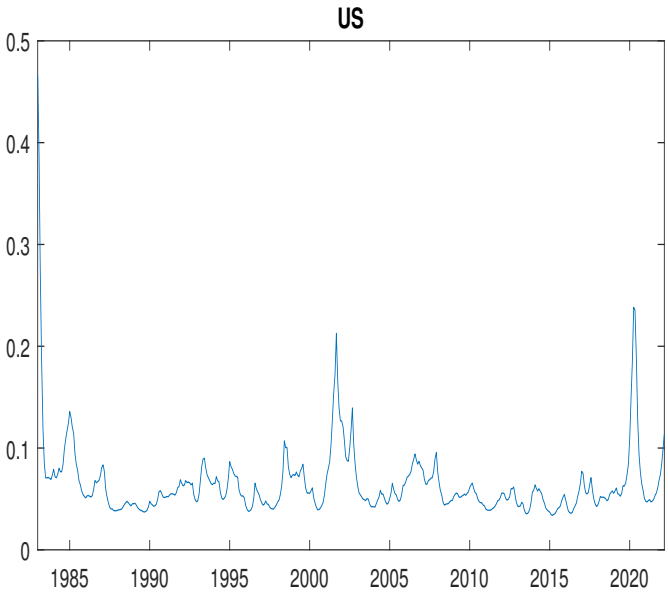

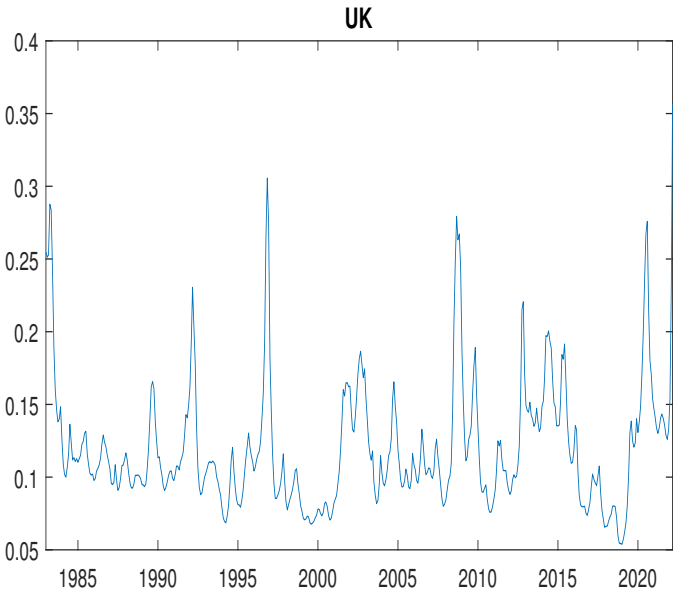

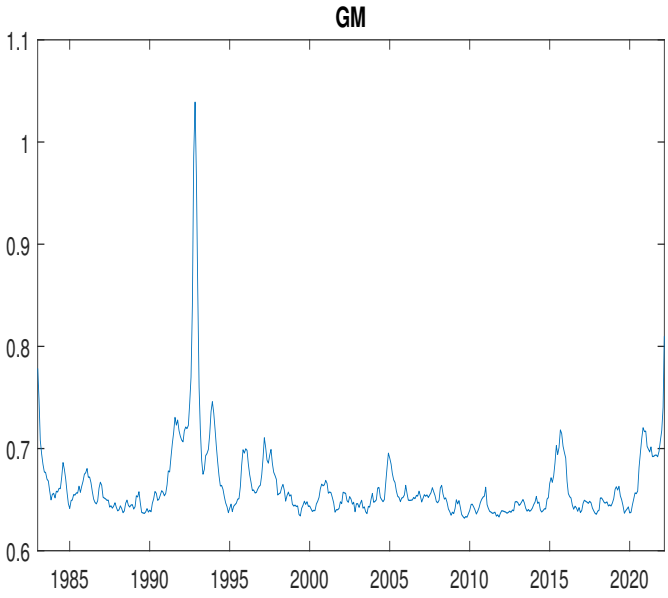

Table 6: **Out-of-sample forecasts for the ten-year forward rate**

Quarterly forecast: 1976Q3-2008Q1	Horizon in quarters				
(127 quarters)	4	10	20	30	40
DTSM with drifting trends (BR)	1.28	1.65	2.25	2.23	2.59
Shadow rate DTSM (SDTSM)	1.11	1.62	2.18	2.19	2.46
p-values: SDTSM≥BR	0.05	0.34	0.23	0.29	0.00

the table is continued on the next page

Quarterly forecast: 1976Q3-2016Q1	Horizon in quarters			
(159 quarters)	1	2	4	8
DTSM with drifting trends (BR)	0.65	0.88	1.21	1.48
Shadow rate DTSM (SDTSM)	0.60	0.74	1.12	1.48
p-values: SDTSM≥BR	0.10	0.01	0.16	0.51

the table is continued on the next page

The standard DTSM has three stationary observed factors which are the first three principal components of yield data. The SDTSM method is our shadow rate DTSM with drifting trends. The BR is the shifting endpoint model in Bauer and Rudebusch (2020). The monthly forecast spans full sample while the quarterly forecast for the U.S. starts in 1971Q4 and ends in 2018Q2. In the upper part of Panel A, the first three rows report the root mean squared errors (RMSE) from different models. The last two rows report p-values of Diebold-Mariano test with the small sample adjustment of Harvey et al. (1997), against the null hypothesis that the SDTSM does not improve the forecast compared with RW, DTSM. The lower part of Panel A follows the same manner comparing SDTSM to BR.